D'Amico *et al. Financial Innovation* (2024) 10:83
https://doi.org/10.1186/s40854-023-00593-0

Financial Innovation

RESEARCH

Open Access

Drawdown-based risk indicators for high-frequency financial volumes

Guglielmo D'Amico[1], Bice Di Basilio[1*] and Filippo Petroni[1]

*Correspondence:
bice.dibasilio@unich.it

[1] Department of Economics, Gabriele D'Annunzio University of Chieti-Pescara, Pescara, Italy

Abstract

In stock markets, trading volumes serve as a crucial variable, acting as a measure for a security's liquidity level. To evaluate liquidity risk exposure, we examine the process of volume drawdown and measures of crash-recovery within fluctuating time frames. These moving time windows shield our financial indicators from being affected by the massive transaction volume, a characteristic of the opening and closing of stock markets. The empirical study is conducted on the high-frequency financial volumes of Tesla, Netflix, and Apple, spanning from April to September 2022. First, we model the financial volume time series for each stock using a semi-Markov model, known as the weighted-indexed semi-Markov chain (WISMC) model. Second, we calculate both real and synthetic drawdown-based risk indicators for comparison purposes. The findings reveal that our risk measures possess statistically different distributions, contingent on the selected time windows. On a global scale, for all assets, financial risk indicators calculated on data derived from the WISMC model closely align with the real ones in terms of Kullback–Leibler divergence.

Keywords: Drawdown-based measures, High-frequency financial volumes, Semi-Markov model, Right censoring, Chi-square independence test, Goodness-of-fit test, Kullback–Leibler divergence

Introduction

In recent years, there has been a growing interest in drawdown-based risk measures within both academic circles and the financial sector, as evidenced by numerous studies (see e.g., D'Amico et al. (2020), D'Amico et al. (2023), Zhang and Hadjiliadis (2012), Hongzhong (YYYY), Li et al. (2022), Jiang (2022), Cantor (2001)). The primary reason for this increased attention is that these measures consider the temporal progression of financial data. This aspect is overlooked by other inflated risk indicators, such as the value-at-risk and the expected shortfall.

Several risk indicators based on drawdown have been proposed in academic literature. Notably, the expected conditional drawdown measures and the conditional drawdown measures are among the most prevalent (e.g., see Goldberg and Mahmoud (2017) and Chekhlov et al. (2005), respectively). This group of financial indicators also includes the maximum drawdown and average drawdown, which are both straightforward and user-friendly (e.g., see Casati and Tabachnik (2013) and Chekhlov et al. (2005), respectively).

Recently, new risk measures based on drawdown, which are closely related to market crashes, have been proposed. Specifically, the drawdown of a fixed level, the time to crash, and the speed of crash were initially introduced in Zhang and Hadjiliadis (2012) and subsequently expanded upon in D'Amico et al. (2020, 2023). These measures provide investors with crucial information about the risk level prior to a crash event occurring. The recovery time and the speed of recovery, which were further developed and examined in D'Amico et al. (2020), examine the phase that transitions an asset from financial collapse to recovery.

To reproduce financial time series, it is necessary to use a stochastic model. There are several models suggested in academic literature, with the most prevalent being econometric models (refer to D'Amico et al. (2023)) or diffusive models (refer to Zhang and Hadjiliadis (2012)). Recently, effective alternatives based on semi-Markovian models have been introduced (refer to D'Amico et al. (2020), Masala and Petroni (2022), Swishchuk and Islam (2011), Swishchuk and Vadori (2017), Vassiliou (2014), Vassiliou (2020), D'Amico and Petroni (2011), D'Amico and Petroni (2012), Limnios and Oprisan (2001), Janssen (2013)).

Semi-Markov processes, which are extensions of Markov processes (refer to Puneet and Dharmaraja (2021), Barbu and Limnios (2009)), describe the time intervals between transitions using any type of distribution. Specifically, a general semi-Markov model, known as the weighted-indexed semi-Markov Chain (WISMC) model, has been used extensively by numerous researchers. It is used in many sectors, including finance, in both its univariate and multivariate versions (see e.g., D'Amico and Petroni (2012), D'Amico and Petroni (2018), De Blasis (2023), Pasricha et al. (2020), D'Amico et al. (2018), D'Amico et al. (2020), Masala and Petroni (2022), D'Amico and Petroni (2021)). The true power of this model, and what distinguishes it from a conventional semi-Markov model, lies in the incorporation of an index process. This process facilitates the aggregation of information derived from the historical trajectory of the financial time series.

This study broadens the scope of all risk measures discussed in D'Amico et al. (2020), including the drawdown of a fixed level, the time to crash, the speed of crash, the recovery time, and the speed of recovery, by considering time-varying windows. Furthermore, it extends their examination to high-frequency financial volumes, given the pivotal role that intraday data play in financial markets, as noted in Zhang et al. (2023). Note that previous studies have consistently applied drawdown-based risk measures to asset returns, not to asset volumes, as seen in D'Amico et al. (2020), D'Amico et al. (2023), Masala and Petroni (2022). Therefore, we posit that incorporating trading volumes into our study represents a novel and original contribution, considering their significant role in stock markets as a key financial quantity for assessing an asset's liquidity risk, as referenced in Queirós (2005), Martınez et al. (2005), Bank et al. (2011). High volumes indicate a liquid asset that can be sold quickly and easily, while low volumes suggest an illiquid asset that is challenging to trade. This demonstrates that WISMC models are suitable for replicating volume data and can thus be effectively employed to study drawdown-based liquidity risk measures.

In this study, we employ a WISMC process to model the minute-by-minute volumes of Tesla, Netflix, and Apple assets listed on the Nasdaq Stock Exchange. First, we verify the need for a model that considers the correlation between transition times and volumes using a χ^2 test. The results consistently reject the independence hypothesis. Second, we calculate drawdown-based risk indicators on both real and synthetic data, which are generated using the WISMC model, in time-varying windows by setting a starting time s. We then conduct a goodness-of-fit test (Song 2002) on the real data to confirm that the selection of different time-varying windows affects our financial indicators, causing them to vary and thus subjecting the investor to fluctuating risk. Third, for both real and simulated financial indicators, we determine their optimal parametric distribution among the Lognormal, Weibull, Exponential, and Gamma laws using the AIC and BIC criteria, as per (D'Amico et al. 2020). This analysis, performed with Type-1 right censorship, is conducted to compare real and simulated risk indicators. Overall, for each asset, the simulated financial risk indicators closely resemble the real ones in terms of Kullback–Leibler divergence.

The structure of the rest of this paper is as follows. In the section titled "Drawdown-based Risk Measures," we offer a detailed explanation of the drawdown-based measures we examine. The "Mathematical Model" tion briefly introduces the WISMC model. In the "Application Results" section, we present the findings of our analysis. Finally, in the "Conclusion" section, we share our final thoughts and objectives for future research.

Drawdown-based risk measures

Trading volumes denote the aggregate count of security transactions within a given time frame, serving as a crucial financial metric that gauges an asset's liquidity. High volumes imply a liquid asset, which can be swiftly sold at the preferred price. Conversely, low volumes suggest an illiquid asset, which poses challenges in converting it into cash. In general, financial volumes are at their peak during the opening and closing of the daily stock market, because traders are required to establish a position. These periods are composed of minutes (refer to Graczyk and Duarte Queiros (2016)). Consequently, we incorporate a general starting time s, which may not necessarily align with the initial minute (i.e., $s = 0$) of the trading day, in the definitions of the risk measures. Therefore, time s enables the computation of all the contemplated financial indicators for any sub-daily interval.

Obviously, if time s equals zero we recover definitions in D'Amico et al. (2020).

To qualify the drawdown of an asset, we introduce the discrete time-varying volume process $X(t)$ and its running maximum process $Y^s(t)$, defined as

$$Y^s(t) := \max_{l \in [s,t]} \{X(l)\}. \tag{1}$$

The introduction of $s > 0$ mitigates the effect of sudden and high initial volume transactions on our risk measures.

Accordingly, the drawdown process $D^s(t)$ is determined as the difference between the running maximum process $Y^s(t)$ and the volume process $X(t)$, as follows:

$$D^s(t) := Y^s(t) - X(t) \text{ with } t \geq s. \tag{2}$$

This expresses the correction of the security trading volume with respect to a previous relative maximum.

To gain a solid understanding of the aforementioned definitions and the function of time s, we provide a visual representation in Fig. 1 for both $s = 0$ and $s = 100$. The red, blue, and black lines depict the volume processes, the ongoing maximum processes, and the drawdown processes, respectively, of the Tesla asset over the course of a trading day. The x-axis denotes the minutes, which serve as the standard unit of measurement for the trading day. Specifically, the stock market day consists of 391 min when $s = 0$, and 291 min when $s = 100$. It is observable that Tesla's volume processes exhibit a characteristic U-shape form (refer to Queirós (2016)), and for $s = 0$, the initial fluctuations are significantly more pronounced than for $s = 100$. Note that substantial and abrupt initial volume changes have significant effects on the calculation of risk measures based on drawdown. Indeed, the running maximum process, and consequently the drawdown process, assume extremely high values from the first few minutes of the trading day.

To examine the influence of these fluctuations on our risk indicators, we calculate them using various starting times s, which represent the point from which the risk measures need to be computed. We introduce drawdown-based financial indicators that are closely related to market crashes, including the drawdown of a fixed level, the time to crash, the speed of crash, the recovery time, and the speed of recovery. These crash-recovery measures are typically applied to financial returns (refer to D'Amico et al. (2020), D'Amico et al. (2023) for examples). However, applying them to trading volumes alters their financial interpretation. Specifically, when volumes are low, these risk measures imply a lack of interest in the asset. On the other hand, high volumes suggest that the security is highly attractive.

The drawdown of fixed level is the first time that the drawdown process achieves or overcomes a certain threshold M.

Rigorously, this is defined as

$$\tau^s(M) := \min\{t \geq s \mid D^s(t) \geq M\} \quad \text{with} \quad M \geq 0. \tag{3}$$

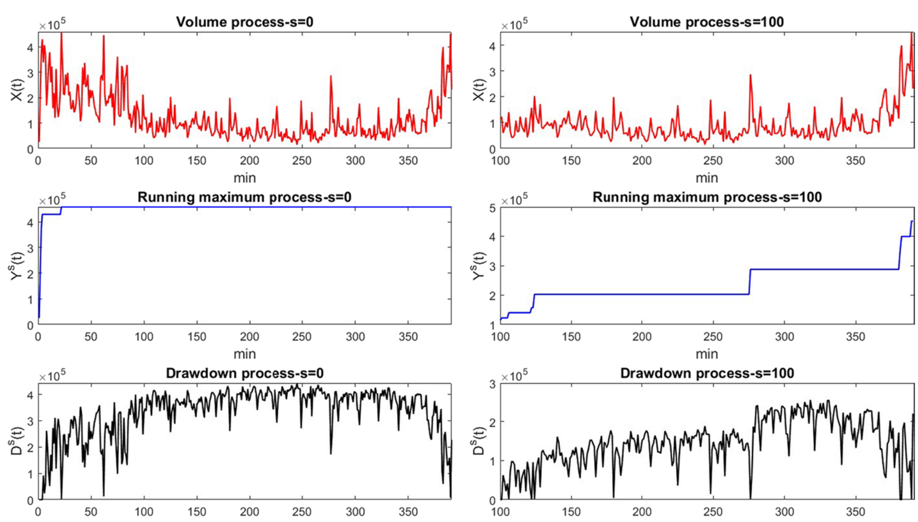

Fig. 1 Volume processes (red lines), running maximum processes (blue lines) and drawdown processes (black lines) for Tesla asset, considering two different starting times ($s = 0$ and $s = 100$)

To identify the time to crash, we need to introduce the last visit time of the maximum before the stopping time $\tau^s(M)$; formally, this is defined as

$$\rho^s(M) := \max\{t \in [s, \tau^s(M)] \mid X(t) = Y^s(t)\}. \tag{4}$$

Exploiting the definition of $\tau^s(M)$ and $\rho^s(M)$, we qualify the time to crash as

$$T_c^s(M) := \tau^s(M) - \rho^s(M). \tag{5}$$

This is the time necessary to have the first M-variation in the drawdown process.

Consequently, the speed of crash, that is, the velocity at which the first M-change occurs, is expressed as

$$S_c^s(M) := \frac{M}{T_c^s(M)}. \tag{6}$$

These indicators offer insights into the level of risk prior to a crash event. Equally, examining the subsequent phase that transitions the financial asset from the crash to recovery is intriguing. In order to do this, we define the quantity $\gamma^s(M, M')$, as follows:

$$\gamma^s(M, M') := \min\{t > \tau^s(M) \mid D^s(t) \leq M'\} \quad \text{with} \quad M > M'. \tag{7}$$

This describes the first moment in which the drawdown process falls below the threshold M', just after having crossed the threshold M for the first time.

Using the definitions of $\gamma^s(M, M')$ and $\tau^s(M)$, the recovery time is determined as

$$R_t^s(M, M') := \gamma^s(M, M') - \tau^s(M). \tag{8}$$

Hence, the speed of recovery, that is, the velocity at which we attain the M' threshold after exceeding the threshold M for the first time, is defined as

$$S_r^s(M, M') := \frac{M - M'}{R_t^s(M, M')}. \tag{9}$$

Figure 2 illustrates graphically all the financial indicators just described, considering Tesla and fixing $s = 100$.

As indicated by the definitions provided, all risk measures depend on a threshold. The risk 'appetite of investors dictates the levels of M and M'. Investors who are more adventurous tend to favor higher thresholds, thereby accepting a higher risk. On the other hand, investors who are more risk-averse opt for lower thresholds, which signifies less risk. However, the selection of these thresholds must be contextualized within the trend of the drawdown process. If the drawdown process exhibits high values and an investor chooses a threshold that is too low, it will be surpassed immediately, placing the investor in a perceived high-risk area. Conversely, if an investor sets a threshold that is too high, there is a possibility that the drawdown will never exceed it, resulting in the stock being perceived as less risky than the investor's maximum 'risk tolerance.

All of these risk indicators provide investors with useful financial tools to evaluate the liquidity risk of a particular investment or investment portfolio. Specifically, τ^s Provides information about the hazard of an asset and depends on the selected M-value. Small M

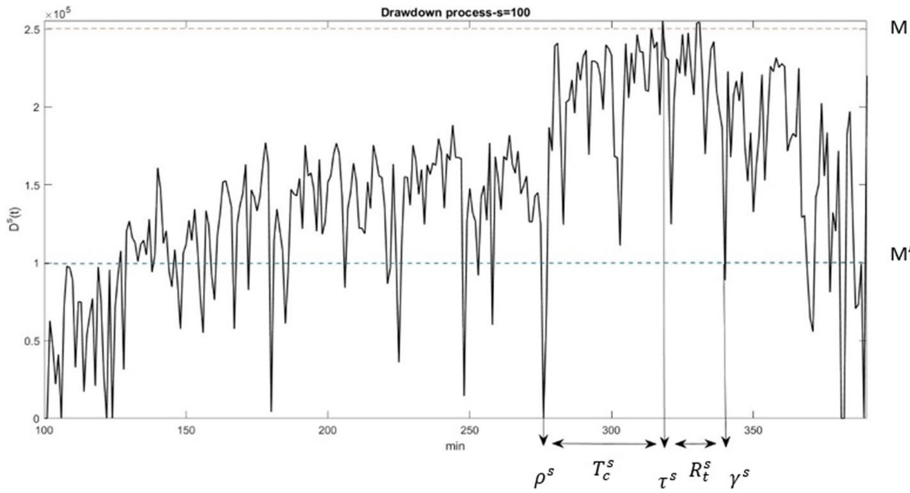

Fig. 2 Drawdown processes of Tesla asset during a trading day, for $s = 100$. The orange and blue lines stand for the thresholds M and M'

values indicate low-risk events, that is, a typical market condition in which the stock can be sold easily (i.e., a liquid asset). Conversely, high M values denote very risky events, signifying very uncertain and unstable market conditions for the asset and, thus, a general difficulty in trading it (i.e., an illiquid asset).

$T_c^s(M)$ and $S_c^s(M)$ quantify how long it takes and how quickly such risky events occur and, consequently, the duration and speed, respectively, at which a stock becomes illiquid.

Unlike previous metrics, $R_t^s(M, M')$ and $S_r^s(M, M')$ examine the behavior of a stock after reaching a specific M-level in its drawdown, thereby indicating a dependency on both the M and M' thresholds. Specifically, the recovery time and the speed of recovery indicate the duration of the drawdown process to reach the M' threshold after already hitting the M threshold, and the rate at which this happens. In simpler terms, these metrics measure the number of minutes an asset requires to shift from an illiquid state to a more liquid one, and the speed of this transition.

Mathematical model

Semi-Markov chain models extend the capabilities of Markov chain models by allowing the time intervals between transitions to be shaped by any given distribution, as opposed to a predetermined one. As such, Markovian processes can be viewed as a specific instance of semi-Markovian processes. This is evident when the waiting time distributions in the states of the system are memoryless distributions, such as the geometric distribution in discrete time or the exponential distribution in continuous time.

Consequently, semi-Markovian models consider the present state of the system and its duration in that state, but they disregard the preceding history. This is a significant limitation for these models, especially because past events are important in financial time series. A potential solution to this problem is the application of a more comprehensive semi-Markov chain model, namely the WISMC model (e.g., D'Amico and Petroni (2012), D'Amico and Petroni (2018), D'Amico and Petroni (2021)).

For this reason, we apply a WISMC process to model the high-frequency financial volumes.

Fundamentally, the WISMC model is described by three stochastic processes: $\{J_n\}_{n\in\mathbb{N}}$, $\{T_n\}_{n\in\mathbb{N}}$, and $\{U_n^\lambda\}_{n\in\mathbb{N}}$, which in our context are the trading volume process, the corresponding jump time process, and the index process, respectively.

Assuming that $X(t)$ is the discrete time-varying volume process of an asset, we transform it into a series of discrete volumes, denoted by $X_d(t)$, following the map described in D'Amico and Petroni (2012). Then, the sequence of discrete volumes $\{X_d(t)\}_{t\in\mathbb{N}}$ is converted into a series of volumes $\{J_n\}_{n\in\mathbb{N}}$, denoting the value of the volumes process at the nth change, and into a series of corresponding jump times $\{T_n\}_{n\in\mathbb{N}}$, signifying the time at which the nth change in the volumes process occurred. In order to do this, we set $T_0 = 0$ and $J_0 = X_d(0)$, and for $n \geq 1$,

$$T_n = \inf\{t \in \mathbb{N}, t > T_{n-1} : X_d(t) \neq X_d(T_{n-1})\}, \tag{10}$$

$$J_n = X_d(T_n). \tag{11}$$

The addition of the stochastic process $\{U_n^\lambda\}_{n\in\mathbb{N}}$, with values in $\mathbb{R}$, is the major extension to the traditional semi-Markov model. The random variable U_n^λ describes the value of the index process at the nth transition, that is, it synthesizes the information contained in the past trajectory of the volume process up to the nth transition. It is defined as

$$U_n^\lambda = \sum_{k=0}^{n-1} \sum_{a=T_{n-1-k}}^{T_{n-k}-1} f^\lambda(J_{n-1-k}, T_n, a) + f^\lambda(J_n, T_n, T_n). \tag{12}$$

To better understand equation (12), we include a numerical example considering only 3 transitions for the volume process (i.e., $n = 3$). In Table 1, we report the volume values ($\{J_0, J_1, J_2, J_3\}$) and the corresponding jump time values ($\{T_0, T_1, T_2, T_3\}$) required in our example.

Note that the volume values in Table 1 are completely unrealistic. We selected them to simplify the notation and thus, construct the example in a functional manner.

By fixing $n = 3$, equation (12) becomes

$$U_3^\lambda = \sum_{k=0}^{2} \sum_{a=T_{2-k}}^{T_{3-k}-1} f^\lambda(J_{2-k}, T_3, a) + f^\lambda(J_3, T_3, T_3).$$

Using data in Table 1, we get

Table 1 Volumes values J_n and corresponding jump times values T_n considering $n = 3$

J_n	T_n
$J_0 = 2$	$T_0 = 0$
$J_1 = 5$	$T_1 = 3$
$J_2 = 3$	$T_2 = 10$
$J_3 = 4$	$T_3 = 50$

$$U_3^\lambda = \sum_{k=0}^{2} \sum_{a=T_{2-k}}^{T_{3-k}-1} f^\lambda(J_{2-k}, 50, a) + f^\lambda(4, 50, 50).$$

Next, we perform the first summation (i.e., the summation with index k), and we obtain

$$U_3^\lambda = \sum_{a=T_2}^{T_3-1} f^\lambda(J_2, 50, a) + \sum_{a=T_1}^{T_2-1} f^\lambda(J_1, 50, a) + \sum_{a=T_0}^{T_1-1} f^\lambda(J_0, 50, a) + f^\lambda(4, 50, 50).$$

Finally, employing numerical values in Table 1, we get

$$U_3^\lambda = \sum_{a=0}^{2} f^\lambda(2, 50, a) + \sum_{a=3}^{9} f^\lambda(5, 50, a) + \sum_{a=10}^{49} f^\lambda(3, 50, a) + f^\lambda(4, 50, 50).$$

Based on previous applications to high-frequency financial data (e.g., D'Amico et al. (2020), D'Amico and Petroni (2018), D'Amico and Petroni (2021)), we employ an exponentially weighted moving average of the squared J as a function f. Formally, we assume the following functional form:

$$f^\lambda(J_{n-1-k}, T_n, a) = \frac{\lambda^{T_n-a} J_{n-1-k}^2}{\sum_{k=0}^{n-1} \sum_{b=T_{n-1-k}}^{T_{n-k}-1} \lambda^{T_n-b}} = \frac{\lambda^{T_n-a} J_{n-1-k}^2}{\sum_{b=1}^{T_n} \lambda^b}. \tag{13}$$

This depends on the past values of volumes J_{n-1-k} that occurred at time a, the current time T_n, and the parameter λ, which balances past information.

In the next section, we describe the calibration of the parameter λ and determining the optimal number of states for the financial volumes, as well as the index process.

To construct the WISMC model, we explicitly define the dependency structure between the random variables J_n, T_n, and U_n^λ. To this end, we adopt the following assumption:

$$\begin{aligned} &\mathbb{P}[J_{n+1} = j,\ T_{n+1} - T_n \le t \mid \sigma(J_h, T_h, U_h^\lambda)_{h=0}^n, J_n = i, U_n^\lambda = u] \\ &\quad = \mathbb{P}[J_{n+1} = j,\ T_{n+1} - T_n \le t \mid J_n = i, U_n^\lambda = u] =: Q_{ij}^\lambda(u, t), \end{aligned} \tag{14}$$

where $\sigma(J_h, T_h, U_h^\lambda)$ is the natural filtration of the three-variate process $\{J_n, T_n, U_n^\lambda\}$. Relation (14) asserts that knowledge of the last volume value ($J_n = i$) and of the value of the index process ($U_n^\lambda = u$) suffices to give the conditional distribution of the couple $(J_{n+1}, T_{n+1} - T_n)$.

In this mathematical model, the matrix of functions $\mathbf{Q}^\lambda(u,t) = (Q_{ij}^\lambda(u,t))_{i,j\in E}$, known as the weighted-indexed semi-Markov kernel, is a crucial component. If $\mathbf{Q}^\lambda(u,t)$ is constant in u, then the weighted-indexed semi-Markov kernel degenerates into a regular semi-Markov kernel.

We denote by $\mathbf{P}^\lambda(u) = (p_{ij}^\lambda(u))_{i,j\in E}$ the transition probabilities of the embedded indexed Markov chain J_n, where

$$p_{ij}^\lambda(u) = \mathbb{P}[J_{n+1} = j \mid J_n = i, U_n^\lambda = u].$$

We assume that $\mathbf{G}^\lambda(u,t) = (G_{ij}^\lambda(u,t))_{ij\in E}$ are the conditional waiting time distribution functions, where

$$G_{ij}^{\lambda}(u,t) = \mathbb{P}[T_{n+1} - T_n \leq t \mid J_n = i, J_{n+1} = j, U_n^{\lambda} = u].$$

Then, equation (14) is equivalent to

$$\begin{aligned} Q_{ij}^{\lambda}(u,t) &= \mathbb{P}[J_{n+1} = j \mid J_n = i, U_n^{\lambda} = u] \cdot \mathbb{P}[T_{n+1} - T_n \leq t \mid J_n = i, J_{n+1} = j, U_n^{\lambda} = u] \\ &= p_{ij}^{\lambda}(u) \cdot G_{ij}^{\lambda}(u,t). \end{aligned}$$

Accordingly, the evolution of the system can be summarized as follows: given a certain state i and a value u of the index process, the transition in the state j is determined using the probability $p_{ij}^{\lambda}(u)$, and the permanence of the system in the state i before moving to state j is determined by using the waiting time distribution function $G_{ij}^{\lambda}(u,t)$.

The triple of processes $\{J_n, T_n, U_n^{\lambda}\}$ describes the system's behavior for the transition time T_n. To characterize the behavior of our model at any time t, which can be a transition time or a waiting time, we must specify additional stochastic processes.

Let $N(t) = \sup\{n \in \mathbb{N} : T_n \leq t\}$ be the number of transitions up to time t, and let $Z(t) = J_{N(t)}$ be the state of the system at time t.

We refer to $Z(t)$ as a weighted indexed semi-Markov process.

For a thorough explanation of the estimation procedures for each quantity included in this model, see D'Amico and Petroni (2018).

Application results

The content of this section is divided into two sub-sections. The first sub-section provides a summary of the key statistical characteristics of the financial data set used in our study, followed by details about the application of the WISMC model. The second subsection discusses the analysis of risk measures, developed using both actual and simulated data.

Data analysis and preliminary model results

The study was conducted using high-frequency trading volumes of three Nasdaq-listed stocks, specifically, Tesla, Netflix, and Apple, which were recorded on a minute-by-minute basis. These corporations were chosen because they represent different industrial sectors. For instance, Tesla is primarily involved in the Automotive and Renewable sector, while Netflix and Apple are part of the Communication Services, Technology & Entertainment, and Information Technology sectors, respectively. The data were sourced from Thomson Reuters EikonTM (https://eikon.thomsonreuters.com/index.html) and covers the period April 2022–September 2022. For each corporation, 49,266 min-by-minute trading volumes were analyzed, corresponding to 126 trading days, with each day comprising 391 min. Table 2 provides the main descriptive statistics of the trading volumes for Tesla, Netflix, and Apple. The results in the table show that Netflix stock seems to have the smallest mean, median, and standard deviation values, but also the largest values of kurtosis and skewness.

In Table 3, using a Jarque–Bera test, we rule out the Gaussian hypothesis for the volumes $X(t)$ at the 1% and 5% significance levels for every asset. The results reject the Gaussian hypothesis for all the considered assets.

Table 2 Mean, median, standard deviation, skewness, and kurtosis of Tesla, Netflix, and Apple volumes

Stock	Mean	Median	SD	Skewness	Kurtosis
TESLA	1.6829e+05	1.3640e+05	1.1824e+05	1.2712	4.5623
NETFLIX	2.1366e+04	15135	1.9718e+04	1.9745	7.5502
APPLE	1.6307e+05	1.3871e+05	1.0125e+05	1.1053	4.3211

Table 3 Jarque-Bera test results performed on Tesla, Netflix, and Apple log-volumes considering both $\alpha = 0.01$ and $\alpha = 0.05$

Stocks	$\alpha = 0.01$	$\alpha = 0.05$
TESLA	Reject H_0	Reject H_0
NETFLIX	Reject H_0	Reject H_0
APPLE	Reject H_0	Reject H_0

Table 4 Contingency table to test the dependence between *X*(*t*) and *T* for Tesla

		$X(t)$				
		$(-\infty, 8] \times 10^4$	$(8, 12] \times 10^4$	$(12, 17) \times 10^4$	$[17, 26) \times 10^4$	$[26, +\infty) \times 10^4$
T	(0, 2]	3129(3567.3)	5947(5740.6)	6136(5750.7)	5487(5286.1)	2666(3020.4)
	(2, 4]	645(456.2)	702(734.1)	580(735.4)	609(676.0)	452(386.3)
	$(4, +\infty)$	433(183.5)	121(295.8)	66(295.8)	138(271.9)	444(155.4)

The numbers in brackets are the theoretical values obtained under the independence hypotheses

Table 5 Contingency table to test the dependence between *X*(*t*) and *T* for Netflix

		$X(t)$				
		$(-\infty, 7.7] \times 10^3$	$(7.7, 12.5] \times 10^3$	$(12.5, 19.5) \times 10^3$	$[19.5, 33) \times 10^3$	$[33, +\infty) \times 10^3$
T	(0, 2]	3204(3538.9)	5649(5385.8)	5899(5566.6)	5056(5027.5)	2344(2633.2)
	(2, 4]	580(471.8)	636(718.0)	627(742.1)	729(670.2)	381(351.0)
	$(4, +\infty)$	424(197.3)	119(300.3)	93(310.3)	193(280.3)	406(146.8)

The numbers in brackets are the theoretical values obtained under the independence hypotheses

Table 6 Contingency table to test the dependence between *X*(*t*) and *T* for Apple

		$X(t)$				
T		$(-\infty, 9] \times 10^4$	$(9, 12.5] \times 10^4$	$(12.5, 17) \times 10^4$	$[17, 25) \times 10^4$	$[25, +\infty) \times 10^4$
	(0, 2]	3015(3405.8)	5572(5345.1)	5792(5429.1)	5085(4983.9)	2439(2739.1)
	(2, 4]	593(477.4)	717(749.2)	627(761.0)	729(698.6)	404(383.9)
	$(4, +\infty)$	484(208.8)	133(327.7)	104(332.7)	174(305.6)	448(168.0)

The numbers in brackets are the theoretical values obtained under the independence hypotheses

Finally, in Tables 4, 5, and 6, we create contingency tables by grouping volumes in five intervals, each containing about 20% of observations. Then, we apply the χ^2 test to check whether the volumes and the waiting times rely on one another. The results show that the independence hypothesis is uniformly rejected by all of the stocks. Specifically, the statistical test scores for Tesla, Netflix, and Apple are 1.4892e+03, 1.1630e+03, and 1.3283e+03, respectively, and 20.0902 is the critical value of the χ^2 statistics with eight degrees of freedom and $\alpha = 0.01$. This is reflected in the low p-values (****).

These arguments highlight the necessity for all assets to adopt a model where the intervals between transitions and volumes are interdependent, and not based on the Gaussian distribution. This necessity prompted us to replicate volumes using a WISMC process.

To properly realize the investigation, we judged real data above the 95th percentile to be outliers, and replaced them with the semi-sum of the nearest data.

In addition, all our high-frequency volumes display a daily pattern, increasing at the opening of the market, decreasing throughout the trading day, and then increasing again at market close. By taking the average for each trading day on a minute-by-minute basis, we establish the daily trend values. To accurately simulate financial volumes using a WISMC model, we removed all trends from the financial time series by modeling these trends with a fourth-degree polynomial. Table 7 shows the estimated coefficient values of the fourth-degree polynomial, along with their respective 95% confidence intervals, for all stocks. The Adjusted-R^2 values of the polynomial regressions are 0.9801, 0.9580, and 0.9677 for Tesla, Netflix, and Apple, respectively.

The WISMC estimations are conducted following the methodology outlined in D'Amico and Petroni (2018). Specifically, to shape volumes using a WISMC process, it is necessary

Table 7 Estimated coefficient values of the fourth-degree polynomial and relative 95% Confidence intervals (95% CI) for Tesla, Netflix, and Apple assets

	Estimated values	**95% CI**
TESLA		
$p1$	0.319×10^4	$(0.187, 0.450) \times 10^4$
$p2$	-0.883×10^4	$(-0.998, -0.769) \times 10^4$
$p3$	3.906×10^4	$(3.555, 4.258) \times 10^4$
$p4$	-2.926×10^4	$(-3.150, -2.701) \times 10^4$
$p5$	12.390×10^4	$(12.220, 12.560) \times 10^4$
NETFLIX		
$p1$	0.147×10^4	$(0.126, 0.168) \times 10^4$
$p2$	0.039×10^4	$(0.021, 0.057) \times 10^4$
$p3$	0.198×10^4	$(0.142, 0.255) \times 10^4$
$p4$	-0.364×10^4	$(-0.401, -0.328) \times 10^4$
$p5$	1.669×10^4	$(1.642, 1.696) \times 10^4$
APPLE		
$p1$	0.900×10^4	$(0.772, 1.029) \times 10^4$
$p2$	0.218×10^4	$(0.106, 0.330) \times 10^4$
$p3$	2.410×10^4	$(2.066, 2.754) \times 10^4$
$p4$	-2.295×10^4	$(-2.514, -2.076) \times 10^4$
$p5$	12.220×10^4	$(12.060, 12.380) \times 10^4$

to establish the number of states for the volume process and the parameter λ for each asset. These two quantities are calibrated by minimizing the mean percentage error between actual and synthetic autocorrelation functions, in line with the algorithm detailed in D'Amico and Petroni (2018). In essence, the algorithm aims to create a trajectory by arbitrarily initiating a set of states and a λ value, estimate the weighted-indexed semi-Markov kernel using the approximate nonparametric maximum likelihood estimator derived in D'Amico et al. (2013), and subsequently conduct a Monte Carlo simulation to generate a synthetic series. The autocorrelation functions for both actual and simulated data are then calculated, and the mean percentage error values are compared. This process is repeated with varying state values and λ. Ultimately, the number of states and the λ value that most accurately represent the data are determined by minimizing the mean percentage error.

Using this optimization procedure, we find that for all stocks, the ideal number of states is five and the optimal value of λ is 0.93. However, note that in previous financial applications, based on the financial returns of other assets, even higher λ values have been observed (see D'Amico and Petroni (2021)).

Specifically, we discretize financial volumes in five states not symmetrical to each other. Denoting as L the detrended financial volume series, we discretize them using the following grid:

$$Mean + Std \cdot [-1, -0.5, 0.5, 1],$$

where $Mean$ and Std are the mean and standard deviation values, respectively, of the L financial time series. The grid detects the following five intervals: $(-\infty, Mean - Std]$, $(Mean - Std, Mean - 0.5 \cdot Std]$, $(Mean - 0.5 \cdot Std, Mean + 0.5 \cdot Std]$, $(Mean + 0.5 \cdot Std, Mean + Std]$, and $(Mean + Std, +\infty)$. The mean and standard deviation values for the detrended volume series for Tesla, Netflix, and Apple are shown in Table 8.

We also discretized the index process into five states: low, medium-low, medium, medium-high, and high volume levels (Fig. 3).

In Figs. 4, 5, and 6, we show the probability plots for both the detrended volumes states and index states for Tesla, Netflix, and Apple, respectively.

Results on drawdown-based risk measures

First, we compute the drawdown-based risk measures using real data. Following this, we examine the hypothesis that different distributions exist as s changes on real risk measures. We do this by employing the goodness-of-fit test suggested in Song (2002). This test, which is grounded in relative entropy or Kullback–Leibler divergence (see Kullback and Leibler (1951)), ascertains whether the distributions of two data sets are statistically identical or not. Formally, the test assumes the following form:

Table 8 Mean and standard deviation values for the detrended series of Tesla, Netflix, and Apple

Stocks	*Mean*	*Std*
TESLA	$2.3772e + 03$	$7.3791e + 04$
NETFLIX	396.5026	$1.0585e + 04$
APPLE	$1.0858e + 03$	$5.9539e + 04$

$$\begin{cases} H_0 : D(P, Q) = 0, \\ H_1 : D(P, Q) > 0. \end{cases} \quad (15)$$

Here, P and Q are two probability distributions, and $D(P, Q)$ indicates their Kullback–Leibler divergence. We define the Kullback–Leibler divergence in its continuous version, denoted also by $D(P\|Q)$, as follows:

$$D(P\|Q) = \int_{-\infty}^{+\infty} p(x) log_2 \left(\frac{p(x)}{q(x)} \right) dx, \quad (16)$$

where p and q are the probability densities of P and Q. This expresses the measure of the information lost when the distribution Q is employed to approximate the distribution P.

Accepting the null hypothesis means stating that we have identical probability distributions, regardless of the starting time s. Conversely, rejecting the null hypothesis implies that we have different probability distributions, both functions of the selected time s.

Practically, we reject H_0 if $Z_0 > z_\alpha$, where $Z_0 = \sqrt{n} \cdot \hat{D}(Q, P)/\hat{\sigma}$, and z_α is the $1 - \alpha$ quantile of the standard normal distribution. For a detailed discussion, see Song (2002); Koukoumis and Karagrigoriou (2021).

Tables 9, 10, 11, 12, 13, 14, 15, 16, 17 show the test results for the measures τ^s, T_c^s, and R_t^s, respectively. Based on the results of the statistical tests, the null hypothesis is nearly always rejected for all securities and risk measures. The significance of this rejection intensifies as the selected s value increases. However, the assumption of distributive equality is occasionally accepted for relatively modest s values, such as $s = 3$ and $s = 5$. Consequently, the chosen time s, representing the point at which an investor takes action, modifies our financial indicators. This causes them to diverge from one another, exposing the investor to varying risks.

Tables 18, 19, 20 show the main descriptive statistics and the number of censored units for the risk measure τ^s for real data on Tesla, Netflix, and Apple, respectively.

Table 9 Song test results for the risk measure τ^s computed on Tesla real data, considering $M = 30\%$, $M = 40\%$, $M = 80\%$. Z_0 is the statistic test value under the null hypothesis

τ^s - TESLA				
$M = 30\%$	**$\alpha = 0.10$**	**$\alpha = 0.05$**	**$\alpha = 0.01$**	**Z_0**
$s = 3$ vs $s = 5$	Reject H_0	Reject H_0	Reject H_0	2.9737
$s = 3$ vs $s = 50$	Reject H_0	Reject H_0	Reject H_0	6.3366
$s = 3$ vs $s = 100$	Reject H_0	Reject H_0	Reject H_0	7.1834
$M = 40\%$	**$\alpha = 0.10$**	**$\alpha = 0.05$**	**$\alpha = 0.01$**	**Z_0**
$s = 3$ vs $s = 5$	Reject H_0	Reject H_0	Reject H_0	2.4755
$s = 3$ vs $s = 50$	Reject H_0	Reject H_0	Reject H_0	5.5628
$s = 3$ vs $s = 100$	Reject H_0	Reject H_0	Reject H_0	7.1885
$M = 80\%$	**$\alpha = 0.10$**	**$\alpha = 0.05$**	**$\alpha = 0.01$**	**Z_0**
$s = 3$ vs $s = 5$	Reject H_0	Reject H_0	Reject H_0	4.8902
$s = 3$ vs $s = 50$	Reject H_0	Reject H_0	Reject H_0	5.8083
$s = 3$ vs $s = 100$	Reject H_0	Reject H_0	Reject H_0	6.3683

Table 10 Song test results for the risk measure τ^s computed on Netflix real data, considering $M = 30\%$, $M = 40\%$, $M = 80\%$. Z_0 is the statistic test value under the null hypothesis

τ^s - NETFLIX				
$M = 30\%$	**$\alpha = 0.10$**	**$\alpha = 0.05$**	**$\alpha = 0.01$**	**Z_0**
$s = 3$ vs $s = 5$	Reject H_0	Reject H_0	Reject H_0	2.7477
$s = 3$ vs $s = 50$	Reject H_0	Reject H_0	Reject H_0	4.2539
$s = 3$ vs $s = 100$	Reject H_0	Reject H_0	Reject H_0	6.9665
$M = 40\%$	**$\alpha = 0.10$**	**$\alpha = 0.05$**	**$\alpha = 0.01$**	**Z_0**
$s = 3$ vs $s = 5$	Reject H_0	Reject H_0	Reject H_0	2.4994
$s = 3$ vs $s = 50$	Reject H_0	Reject H_0	Reject H_0	4.0489
$s = 3$ vs $s = 100$	Reject H_0	Reject H_0	Reject H_0	4.0882
$M = 80\%$	**$\alpha = 0.10$**	**$\alpha = 0.05$**	**$\alpha = 0.01$**	**Z_0**
$s = 3$ vs $s = 5$	Reject H_0	Reject H_0	Reject H_0	5.1460
$s = 3$ vs $s = 50$	Reject H_0	Reject H_0	Reject H_0	5.2002
$s = 3$ vs $s = 100$	Reject H_0	Reject H_0	Reject H_0	5.1509

Table 11 Song test results for the risk measure τ^s computed on Apple real data, considering $M = 30\%$, $M = 40\%$, $M = 80\%$. Z_0 is the statistic test value under the null hypothesis

τ^s - APPLE				
$M = 30\%$	**$\alpha = 0.10$**	**$\alpha = 0.05$**	**$\alpha = 0.01$**	**Z_0**
$s = 3$ vs $s = 5$	Reject H_0	Reject H_0	Reject H_0	2.8595
$s = 3$ vs $s = 50$	Reject H_0	Reject H_0	Reject H_0	4.2746
$s = 3$ vs $s = 100$	Reject H_0	Reject H_0	Reject H_0	4.4523
$M = 40\%$	**$\alpha = 0.10$**	**$\alpha = 0.05$**	**$\alpha = 0.01$**	**Z_0**
$s = 3$ vs $s = 5$	Reject H_0	Reject H_0	Accept H_0	2.1057
$s = 3$ vs $s = 50$	Reject H_0	Reject H_0	Reject H_0	4.1383
$s = 3$ vs $s = 100$	Reject H_0	Reject H_0	Reject H_0	5.2446
$M = 80\%$	**$\alpha = 0.10$**	**$\alpha = 0.05$**	**$\alpha = 0.01$**	**Z_0**
$s = 3$ vs $s = 5$	Reject H_0	Reject H_0	Reject H_0	5.7759
$s = 3$ vs $s = 50$	Reject H_0	Reject H_0	Reject H_0	6.3895
$s = 3$ vs $s = 100$	Reject H_0	Reject H_0	Reject H_0	6.9665

The mean and standard deviation estimates are obtained using the Kaplan–Meier estimator (Kaplan and Meier 1958) in order to treat the censored units. Recall that the risk measures τ^s, T_c^s, and R_t^s are right-censored, owing to the choice of a fixed observation time, namely, the trading day consisting of 391 min. For an extensive description of the Type-1 right censorship issue and the drawdown-based measures used in this study, see D'Amico et al. (2020).

In terms of the mean value, for each s, all stocks display a comparable trend, with only a few deviations, implying that more severe events occur at a slower pace, and hence, it requires more time for an asset to become highly illiquid. For instance, in the case of Tesla, when $s = 50$, a drawdown variation of 30% is typically reached just

Table 12 Song test results for the risk measure T_c^s computed on Tesla real data, considering $M = 30\%$, $M = 40\%$, $M = 80\%$. Z_0 is the statistic test value under the null hypothesis

T_c^s - TESLA				
$M = 30\%$	**$\alpha = 0.10$**	**$\alpha = 0.05$**	**$\alpha = 0.01$**	**Z_0**
$s = 3$ vs $s = 5$	Reject H_0	Reject H_0	Reject H_0	2.5728
$s = 3$ vs $s = 50$	Reject H_0	Reject H_0	Reject H_0	4.4457
$s = 3$ vs $s = 100$	Reject H_0	Reject H_0	Reject H_0	5.1748
$M = 40\%$	**$\alpha = 0.10$**	**$\alpha = 0.05$**	**$\alpha = 0.01$**	**Z_0**
$s = 3$ vs $s = 5$	Reject H_0	Reject H_0	Reject H_0	4.3123
$s = 3$ vs $s = 50$	Reject H_0	Reject H_0	Reject H_0	4.4484
$s = 3$ vs $s = 100$	Reject H_0	Reject H_0	Reject H_0	5.4716
$M = 80\%$	**$\alpha = 0.10$**	**$\alpha = 0.05$**	**$\alpha = 0.01$**	**Z_0**
$s = 3$ vs $s = 5$	Reject H_0	Reject H_0	Reject H_0	3.4264
$s = 3$ vs $s = 50$	Reject H_0	Reject H_0	Reject H_0	5.5782
$s = 3$ vs $s = 100$	Reject H_0	Reject H_0	Reject H_0	6.0178

Table 13 Song test results for the risk measure T_c^s computed on Netflix real data, considering $M = 30\%$, $M = 40\%$, $M = 80\%$. Z_0 is the statistic test value under the null hypothesis

T_c^s - NETFLIX				
$M = 30\%$	**$\alpha = 0.10$**	**$\alpha = 0.05$**	**$\alpha = 0.01$**	**Z_0**
$s = 3$ vs $s = 5$	Reject H_0	Accept H_0	Accept H_0	1.4045
$s = 3$ vs $s = 50$	Reject H_0	Reject H_0	Reject H_0	2.3998
$s = 3$ vs $s = 100$	Reject H_0	Reject H_0	Reject H_0	2.6583
$M = 40\%$	**$\alpha = 0.10$**	**$\alpha = 0.05$**	**$\alpha = 0.01$**	**Z_0**
$s = 3$ vs $s = 5$	Reject H_0	Accept H_0	Accept H_0	1.5705
$s = 3$ vs $s = 50$	Reject H_0	Reject H_0	Reject H_0	2.6412
$s = 3$ vs $s = 100$	Reject H_0	Reject H_0	Reject H_0	3.1388
$M = 80\%$	**$\alpha = 0.10$**	**$\alpha = 0.05$**	**$\alpha = 0.01$**	**Z_0**
$s = 3$ vs $s = 5$	Reject H_0	Reject H_0	Reject H_0	2.8986
$s = 3$ vs $s = 50$	Reject H_0	Reject H_0	Reject H_0	4.8826
$s = 3$ vs $s = 100$	Reject H_0	Reject H_0	Reject H_0	5.0606

before the second minute. However, to witness a significant shift, such as 80%, we need to wait longer, approximately 14 min, on average.

For all three assets, we simulate daily volumes using the WISMC model, and then compute the analyzed risk indicators for these synthetic series.

Given the real and simulated measures, we can estimate their best parametric distribution among the lognormal, Weibull, exponential, and gamma laws by using the AIC and BIC, according to D'Amico et al. (2020). For the measure T_c^s, we choose the model with the smallest AIC and BIC values, fixing s and varying M. We repeat the same steps for the measure R_t^s, setting s and M, while varying M'. All estimation procedures involving parametric models are performed in Matlab software, considering the right censoring issue.

Table 14 Song test results for the risk measure T_c^s computed on Apple real data, considering $M = 30\%$, $M = 40\%$, $M = 80\%$. Z_0 is the statistic test value under the null hypothesis

T_c^s - APPLE				
$M = 30\%$	$\alpha = 0.10$	$\alpha = 0.05$	$\alpha = 0.01$	Z_0
$s = 3$ vs $s = 5$	Reject H_0	Reject H_0	Accept H_0	1.8749
$s = 3$ vs $s = 50$	Reject H_0	Reject H_0	Reject H_0	3.5555
$s = 3$ vs $s = 100$	Reject H_0	Reject H_0	Reject H_0	3.0716
$M = 40\%$	$\alpha = 0.10$	$\alpha = 0.05$	$\alpha = 0.01$	Z_0
$s = 3$ vs $s = 5$	Reject H_0	Accept H_0	Accept H_0	1.3535
$s = 3$ vs $s = 50$	Reject H_0	Reject H_0	Reject H_0	3.1472
$s = 3$ vs $s = 100$	Reject H_0	Reject H_0	Reject H_0	3.8527
$M = 80\%$	$\alpha = 0.10$	$\alpha = 0.05$	$\alpha = 0.01$	Z_0
$s = 3$ vs $s = 5$	Reject H_0	Reject H_0	Reject H_0	4.4914
$s = 3$ vs $s = 50$	Reject H_0	Reject H_0	Reject H_0	5.9966
$s = 3$ vs $s = 100$	Reject H_0	Reject H_0	Reject H_0	6.6413

Table 15 Song test results for the risk measure R_t^s computed on Tesla real data, fixing $M = 80\%$ and considering $M' = 30\%$, $M' = 40\%$, $M' = 50\%$. Z_0 is the statistic test value under the null hypothesis

R_t^s - TESLA				
$M = 80\% - M' = 30\%$	$\alpha = 0.10$	$\alpha = 0.05$	$\alpha = 0.01$	Z_0
$s = 3$ vs $s = 5$	Reject H_0	Reject H_0	Reject H_0	3.3237
$s = 3$ vs $s = 50$	Reject H_0	Reject H_0	Reject H_0	3.5664
$s = 3$ vs $s = 100$	Reject H_0	Reject H_0	Reject H_0	3.7879
$M = 80\% - M' = 40\%$	$\alpha = 0.10$	$\alpha = 0.05$	$\alpha = 0.01$	Z_0
$s = 3$ vs $s = 5$	Reject H_0	Reject H_0	Reject H_0	2.6889
$s = 3$ vs $s = 50$	Reject H_0	Reject H_0	Reject H_0	3.0386
$s = 3$ vs $s = 100$	Reject H_0	Reject H_0	Reject H_0	3.1136
$M = 80\% - M' = 50\%$	$\alpha = 0.10$	$\alpha = 0.05$	$\alpha = 0.01$	Z_0
$s = 3$ vs $s = 5$	Reject H_0	Reject H_0	Reject H_0	2.7205
$s = 3$ vs $s = 50$	Reject H_0	Reject H_0	Reject H_0	5.0314
$s = 3$ vs $s = 100$	Reject H_0	Reject H_0	Reject H_0	4.9808

Tables 21, 22, 23, 24, 25, 26, 27, 28, 29, 30, 31, 32 show the parametric model selections for the measures T_c^s and R_t^s, respectively. The smallest AIC and BIC values are shown in bold. For both real and simulated data, the lognormal law is invariably the best statistical parametric model. This result underlines the fact that the WISMC model exhibits steady outcomes, consistent with real data, and in line with the findings of D'Amico et al. (2020) in terms of financial returns.

Accordingly, Tables 33, 34, 35, 36, 37, 38 show the parameter point estimates of the best-selected models for the time to crash T_c^s and the recovery time R_t^s, respectively.

We can obtain the best parametric distributions of S_c^s and S_r^s from the best T_c^s and R_t^s parametric distributions, respectively, because S_c^s and S_r^s are their nonlinear

Table 16 Song test results for the risk measure R_t^s computed on Netflix real data, fixing $M = 80\%$ and considering $M' = 30\%$, $M' = 40\%$, $M' = 50\%$. Z_0 is the statistic test value under the null hypothesis

R_t^s - NETFLIX				
$M = 80\% - M' = 30\%$	$\alpha = 0.10$	$\alpha = 0.05$	$\alpha = 0.01$	Z_0
$s = 3$ vs $s = 5$	Reject H_0	Reject H_0	Reject H_0	4.0946
$s = 3$ vs $s = 50$	Reject H_0	Reject H_0	Reject H_0	4.1780
$s = 3$ vs $s = 100$	Reject H_0	Reject H_0	Reject H_0	4.5418
$M = 80\% - M' = 40\%$	$\alpha = 0.10$	$\alpha = 0.05$	$\alpha = 0.01$	Z_0
$s = 3$ vs $s = 5$	Reject H_0	Reject H_0	Reject H_0	3.9262
$s = 3$ vs $s = 50$	Reject H_0	Reject H_0	Reject H_0	2.9611
$s = 3$ vs $s = 100$	Reject H_0	Reject H_0	Reject H_0	4.2846
$M = 80\% - M' = 50\%$	$\alpha = 0.10$	$\alpha = 0.05$	$\alpha = 0.01$	Z_0
$s = 3$ vs $s = 5$	Reject H_0	Reject H_0	Reject H_0	3.1574
$s = 3$ vs $s = 50$	Reject H_0	Reject H_0	Reject H_0	3.2756
$s = 3$ vs $s = 100$	Reject H_0	Reject H_0	Reject H_0	3.9193

Table 17 Song test results for the risk measure R_t^s computed on Apple real data, fixing $M = 80\%$ and considering $M' = 30\%$, $M' = 40\%$, $M' = 50\%$. Z_0 is the statistic test value under the null hypothesis

R_t^s - APPLE				
$M = 80\% - M' = 30\%$	$\alpha = 0.10$	$\alpha = 0.05$	$\alpha = 0.01$	Z_0
$s = 3$ vs $s = 5$	Reject H_0	Reject H_0	Reject H_0	3.5914
$s = 3$ vs $s = 50$	Reject H_0	Reject H_0	Reject H_0	3.6174
$s = 3$ vs $s = 100$	Reject H_0	Reject H_0	Reject H_0	3.9189
$M = 80\% - M' = 40\%$	$\alpha = 0.10$	$\alpha = 0.05$	$\alpha = 0.01$	Z_0
$s = 3$ vs $s = 5$	Reject H_0	Reject H_0	Reject H_0	3.5217
$s = 3$ vs $s = 50$	Reject H_0	Reject H_0	Reject H_0	3.6957
$s = 3$ vs $s = 100$	Reject H_0	Reject H_0	Reject H_0	3.4733
$M = 80\% - M' = 50\%$	$\alpha = 0.10$	$\alpha = 0.05$	$\alpha = 0.01$	Z_0
$s = 3$ vs $s = 5$	Reject H_0	Reject H_0	Reject H_0	3.2731
$s = 3$ vs $s = 50$	Reject H_0	Reject H_0	Reject H_0	3.3765
$s = 3$ vs $s = 100$	Reject H_0	Reject H_0	Reject H_0	3.1379

transformations. All mathematical steps used to derive the two speeds' best parametric distributions from the best T_c^s and R_t^s are reported in D'Amico et al. (2020).

In Tables 39, 40, 41, we present both the main descriptive statistics and the number of censored units for the time to crash T_c^s for Tesla, Netflix, and Apple stocks. The computation is carried out on real data, using the best statistical parametric model as a function of the threshold M. For every s, we observe that the average values and the standard deviation values increase with M. For Tesla and Apple, there are no censored units, but Netflix shows slight censorship for every s. For context, considering Tesla at $s = 50$, a 30% change in its drawdown, occurs in less than two minutes, on average, while an 80% variation is reached in about three minutes, on average. In other words, it takes Tesla

Table 18 Descriptive statistics of τ^s (first quartile, second quartile (median), third quartile, mean, standard deviation, asymmetry index) and related censored unit as a function of the threshold M

Descriptive statistics of τ^s-TESLA							
$s = 0$(%)	**Q1**	**Q2**	**Q3**	**Mean**	**SD**	**AI**	**Censoring rate (%)**
$M = 30$	5	7	11	6.3770	7.7314	-0.2417	0
$M = 40$	5	7	11	6.4524	7.7553	-0.2118	0
$M = 80$	5	7	12	5.0397	8.6643	-0.6788	0
$s = 5$ (%)	**Q1**	**Q2**	**Q3**	**Mean**	**SD**	**AI**	**Censoring rate (%)**
$M = 30$	4	8	12	6.9167	8.4828	-0.3831	0
$M = 40$	4	10	16	8.8095	11.4713	-0.3113	0
$M = 80$	18	30	54	34.6032	30.5603	0.4519	0
$s = 50$ (%)	**Q1**	**Q2**	**Q3**	**Mean**	**SD**	**AI**	**Censoring rate (%)**
$M = 30$	3	4	5	1.8214	3.3564	-1.9472	0
$M = 40$	3	5	7	2.9385	4.5669	-1.3581	0
$M = 80$	6	11	23	14.4643	20.6719	0.5028	0
$s = 100$ (%)	**Q1**	**Q2**	**Q3**	**Mean**	**SD**	**AI**	**Censoring rate (%)**
$M = 30$	3	3.5	5	1.3730	2.7824	-2.2933	0
$M = 40$	3	4	5	1.8214	3.2823	-1.9912	0
$M = 80$	5	8.5	17	9.6667	14.4247	0.2426	0

All results refer to Tesla real data

much longer to achieve a more illiquid position, that is, an 80%-drawdown variation, than to achieve a more liquid one, that is, a 30%-drawdown variation.

Given that we know the cumulative distribution function and the probability distribution function for the time to crash in the most effective statistical parametric models, we can convert these results to the speed of crash, which is a nonlinear transformation of the original data. The mathematical calculations needed to derive the cumulative distribution function and probability distribution function for the speed of crash from the time to crash data are reported in D'Amico et al. (2020). Tables 42, 43, 44 show the main descriptive statistics and the censoring rate for S_c^s. Note that when M rises, the average speed drops. This means that all stocks approach higher thresholds more slowly than they do lower ones, gradually transitioning from a liquid to an illiquid state. Using Tesla as an example, when $s = 50$, a 30% change in its drawdown is reached with an average velocity of 0.1232 min^{-1}, while a bigger variation, such as 80%, is attained more slowly, with an average speed of 0.2883 min^{-1}.

We display the main descriptive statistics and the censoring rate for the measure R_t^s in Tables 45, 46, 47. We observe that fixing M', for each s, if M increases, then the mean value, the standard deviation value, and the censoring rate decrease. In particular, the behavior of the average values of R_t^s emphasizes that after experiencing an 80%-liquidity drop (i.e., $M = 80\%$), all the considered assets need fewer minutes, on average, to recover a more liquid position (i.e., high M' values, and thus small $M - M'$) than they for an illiquid position (i.e., small M' values, and thus high $M - M'$).

Table 19 Descriptive statistics of τ^s (First Quartile, Second Quartile (Median), Third Quartile, Mean, Standard Deviation, Asymmetry Index) and related censored units as a function of the threshold *M*. All results refer to Netflix real data

Descriptive statistics of τ^s-NETFLIX							
$s = 0$ (%)	**Q1**	**Q2**	**Q3**	**Mean**	**SD**	**AI**	**Censoring rate (%)**
$M = 30$	4	5	6	4.7302	20.3237	-0.0398	0
$M = 40$	4	5	6	4.9722	23.4389	-0.0036	0
$M = 80$	4	5	6	4.2302	13.5855	-0.1700	0.8
$s = 5$ (%)	**Q1**	**Q2**	**Q3**	**Mean**	**SD**	**AI**	**Censoring rate (%)**
$M = 30$	3	4	6	6.1230	21.4727	0.2966	0
$M = 40$	4	5	8	7.7857	25.6596	0.3257	0
$M = 80$	8	13	30	20.3571	31.6203	0.6980	0.8
$s = 50$	**Q1**	**Q2**	**Q3**	**Mean**	**SD**	**AI**	**Censoring rate (%)**
$M = 30$	3	4	5	3.4325	11.4496	-0.1102	0
$M = 40$	3	4	5	4.7421	20.2230	0.1102	0
$M = 80$	5	8	15	12.5754	26.0906	0.5261	1.6
$s = 100$ (%)	**Q1**	**Q2**	**Q3**	**Mean**	**SD**	**AI**	**Censoring rate (%)**
$M = 30$	3	3.5	5	2.6865	11.5271	-0.2117	0
$M = 40$	3	4	5	3.3571	14.9780	-0.1288	0
$M = 80$	5	8	14	9.4048	16.9184	0.2491	1.6

Once the speed of recovery S_r^s is a nonlinear transformation of the recovery time R_t^s, we derive its cumulative distribution function and probability distribution function from those of R_t^s, following (D'Amico et al. 2020). Tables 48, 49, 50 report the descriptive statistics and the censoring rate for the measure S_r^s, which denotes the velocity at which a stock goes from an illiquid state to a more liquid state. Note that for Netflix, when fixing s and M' and increasing M, the mean value, the standard deviation, and the censorship rate decrease. Apple shows the same behavior, except for its mean values when $s = 5$. Finally, Tesla always follows this pattern for the standard deviation values, but not for its average values when $s = 5$ and $s = 50$.

To measure the distance between real and simulated measures, we compute the Kullback–Leibler divergence (Kullback and Leibler 1951) for T_c^s and R_t^s.

Table 51 shows the Kullback–Leibler divergences for the time to crash T_c^s while, in Table 52, we present finding values of the recovery time R_t^s. The shortest distances for each s are shown in bold.

Because the Kullback–Leibler divergence is invariant with regard to parameter transformations, its computation is not needed for S_c^s and S_r^s (see D'Amico et al. (2020)).

For T_c^s, note that between the smallest distances highlighted in bold, the greatest distance always occurs for $s = 0$ for each security. Conversely, for R_t^s, the greatest distance between the smaller ones varies for $s = 5$ for both Tesla and Apple, but for Netflix, this occurs when $s = 0$.

Table 20 Descriptive statistics of τ^s (First Quartile, Second Quartile (Median), Third Quartile, Mean, Standard Deviation, Asymmetry Index) and related censored units as a function of the threshold M. All results refer to Apple real data

Descriptive statistics of τ^s-APPLE							
$s = 0$ (%)	**Q1**	**Q2**	**Q3**	**Mean**	**SD**	**AI**	**Censoring rate (%)**
$M = 30$	2	4	5	2.7500	7.0612	-0.5311	0
$M = 40$	2	4	5	2.8413	7.2456	-0.4798	0
$M = 80$	2	4	5	3.4444	8.4238	-0.9101	0
$s = 5$ (%)	**Q1**	**Q2**	**Q3**	**Mean**	**SD**	**AI**	**Censoring rate (%)**
$M = 30$	4	5	8	4.4048	7.4041	-0.2412	0
$M = 40$	4	7	10	5.8849	8.1405	-0.4109	0
$M = 80$	14	27.5	56	35.9087	38.4186	0.6566	0
$s = 50$ (%)	**Q1**	**Q2**	**Q3**	**Mean**	**SD**	**AI**	**Censoring rate (%)**
$M = 30$	3	4	5	1.9966	3.4151	-1.7604	0
$M = 40$	3	4	6	3.2262	4.8787	-1.0907	0
$M = 80$	8	14	26	21.4246	32.8473	0.6781	1.6
$s = 100$ (%)	**Q1**	**Q2**	**Q3**	**Mean**	**SD**	**AI**	**Censoring rate (%)**
$M = 30$	3	4	5	1.9286	3.2494	-1.9125	0
$M = 40$	4	5	6	2.7659	4.0753	-1.6446	0
$M = 80$	8	12.5	25	15.9048	22.4812	0.4543	0

Table 21 Selection of the best parametric model as a function of s and M for the measure T_c^s computed on Tesla real data

Model selection for T_c^s-TESLA								
	Lognormal		**Exponential**		**Weibull**		**Gamma**	
$M \mid s = 0$	**AIC**	**BIC**	**AIC**	**BIC**	**AIC**	**BIC**	**AIC**	**BIC**
30%	**110.75732**	**116.4299**	299.6115	302.4478	239.4154	245.0880	175.9924	181.6650
40%	**140.6871**	**146.3595**	309.4309	312.2672	254.3569	260.0294	200.2211	205.8926
80%	**168.6363**	**174.3090**	320.4233	323.2596	274.7377	280.4103	227.1266	232.7991
$M \mid s = 5$	**AIC**	**BIC**	**AIC**	**BIC**	**AIC**	**BIC**	**AIC**	**BIC**
30%	**537.2757**	**542.9483**	571.9717	574.8080	567.9691	573.6417	561.2803	566.9529
40%	**667.2019**	**672.8744**	695.6664	698.5027	697.5667	703.2393	697.0157	702.6882
80%	**739.0992**	**744.7717**	753.6258	756.4621	755.4354	761.1079	754.4520	760.1245
$M \mid s = 50$	**AIC**	**BIC**	**AIC**	**BIC**	**AIC**	**BIC**	**AIC**	**BIC**
30%	**296.8324**	**302.5049**	395.5940	398.4302	354.4324	360.1050	327.5050	333.1736
40%	**398.1545**	**403.8270**	466.6605	469.4967	457.7519	463.4244	439.7508	445.4234
80%	**490.9344**	**496.6069**	544.4752	547.3115	544.8708	550.5434	536.4257	542.0982
$M \mid s = 100$	**AIC**	**BIC**	**AIC**	**BIC**	**AIC**	**BIC**	**AIC**	**BIC**
30%	**156.3761**	**162.0486**	321.9552	324.7915	229.0281	234.7007	187.0436	192.7161
40%	**246.7348**	**252.4074**	366.6243	369.4606	292.5898	298.2623	267.9816	273.6541
80%	**348.9166**	**354.5892**	428.6731	431.5094	397.4486	403.1212	376.5227	382.2003

The best parametric model is chosen by means of the AIC and BIC criteria. The smallest AIC and BIC values are in bold

Table 22 Selection of the best parametric model as a function of s and M for the measure T_c^s computed on Netflix real data

Model selection for T_c^s-NETFLIX								
	Lognormal		**Exponential**		**Weibull**		**Gamma**	
$M \mid s = 0$	**AIC**	**BIC**	**AIC**	**BIC**	**AIC**	**BIC**	**AIC**	**BIC**
30%	**214.8728**	**220.5454**	397.8642	400.7005	391.7151	397.3876	397.3270	402.9996
40%	**239.5499**	**245.2224**	458.7985	461.6347	423.4447	429.1172	458.1477	463.8203
80%	**290.7235**	**296.3961**	807.2353	810.0716	499.1320	504.8046	634.9171	640.5896
$M \mid s = 5$	**AIC**	**BIC**	**AIC**	**BIC**	**AIC**	**BIC**	**AIC**	**BIC**
30%	**465.3088**	**470.9813**	560.9757	563.8120	551.4480	557.1206	562.6032	568.2758
40%	**516.3383**	**522.0108**	606.3285	609.1647	595.2202	600.9277	607.8449	613.5174
80%	**625.0440**	**630.7166**	886.3748	889.2111	723.3731	729.0456	806.3157	811.9883
$M \mid s = 50$	**AIC**	**BIC**	**AIC**	**BIC**	**AIC**	**BIC**	**AIC**	**BIC**
30%	**347.7825**	**353.4550**	482.4938	485.3300	471.1201	476.7927	484.4893	490.1619
40%	**411.3672**	**417.0398**	549.4779	552.3142	523.5930	529.2656	548.3202	553.9927
80%	**472.9047**	**478.5772**	843.5308	846.3671	612.1396	617.8121	720.6387	726.3113
$M \mid s = 100$	**AIC**	**BIC**	**AIC**	**BIC**	**AIC**	**BIC**	**AIC**	**BIC**
30%	**282.1726**	**287.8452**	424.6410	427.4773	424.5338	430.2064	418.8807	424.5532
40%	**347.8117**	**353.4842**	500.4179	503.2541	484.4048	490.0773	502.4159	508.0884
80%	**424.3772**	**430.0498**	825.0327	827.8689	585.6312	591.3037	702.1969	707.8695

The best parametric model is chosen by means of the AIC and BIC criteria. The smallest AIC and BIC values are in bold

Table 23 Selection of the best parametric model as a function of s and M for the measure T_c^s computed on Apple real data

Model selection for T_c^s-APPLE								
	Lognormal		**Exponential**		**Weibull**		**Gamma**	
$M \mid s = 0$	**AIC**	**BIC**	**AIC**	**BIC**	**AIC**	**BIC**	**AIC**	**BIC**
30%	**-112.2244**	**-106.5518**	265.7230	268.5593	17.0933	22.7658	-84.5238	-78.8513
40%	**8.0156**	**13.6881**	278.7444	281.5807	190.5006	196.1732	82.5840	88.2566
80%	**81.9986**	**87.6712**	294.5545	297.3907	237.1486	242.8212	159.5677	165.2403
$M \mid s = 5$	**AIC**	**BIC**	**AIC**	**BIC**	**AIC**	**BIC**	**AIC**	**BIC**
30%	**406.3261**	**411.9987**	468.3747	471.2110	453.495	459.1683	438.1868	443.8593
40%	**504.0726**	**509.7451**	540.7451	543.4933	533.7475	539.4201	526.7935	532.4661
80%	**583.2903**	**588.9629**	604.8417	607.6780	602.66411	608.3367	599.3333	605.0058
$M \mid s = 50$	**AIC**	**BIC**	**AIC**	**BIC**	**AIC**	**BIC**	**AIC**	**BIC**
30%	**238.4327**	**244.1052**	362.7572	365.5935	294.2205	299.8931	263.9826	269.6551
40%	**374.5056**	**380.1782**	446.9909	449.8272	433.2030	438.8755	414.3182	419.9907
80%	**498.2699**	**503.9424**	543.2089	546.0452	539.6829	545.3555	530.8939	536.5664
$M \mid s = 100$	**AIC**	**BIC**	**AIC**	**BIC**	**AIC**	**BIC**	**AIC**	**BIC**
30%	**272.0607**	**277.7332**	377.8818	380.7180	318.0543	323.7269	295.4658	301.1384
40%	**353.3743**	**359.0469**	428.6731	431.5094	393.5341	399.2040	376.7863	382.4589
80%	**441.8475**	**447.5200**	494.3269	497.1632	483.6473	489.3199	471.9262	477.5988

The best parametric model is chosen by means of the AIC and BIC criteria. The smallest AIC and BIC values are in bold

Table 24 Selection of the best parametric model as a function of s and M for the measure T_c^s computed on Tesla simulated data

Model selection for T_c^s-simulated data for Tesla								
	Lognormal		**Exponential**		**Weibull**		**Gamma**	
$M \mid s = 0$	**AIC**	**BIC**	**AIC**	**BIC**	**AIC**	**BIC**	**AIC**	**BIC**
30%	**416.0895**	**421.7621**	474.2846	477.120	465.6829	471.3555	452.4793	458.1518
40%	**484.7729**	**490.4455**	534.1618	536.9981	535.0857	540.7582	528.5053	534.1779
80%	**582.0063**	**587.6789**	625.3534	628.1926	626.0465	631.7191	627.2512	632.9237
$M \mid s = 5$	**AIC**	**BIC**	**AIC**	**BIC**	**AIC**	**BIC**	**AIC**	**BIC**
30%	**439.012**	**444.7438**	494.3269	497.1632	488.5368	494.1993	476.9298	482.6024
40%	**511.9689**	**517.6415**	549.4779	552.3142	548.0072	553.6797	542.2484	547.9209
80%	**592.8549**	**598.5274**	627.6369	630.4732	629.6316	635.3041	627.7950	633.4676
$M \mid s = 50$	**AIC**	**BIC**	**AIC**	**BIC**	**AIC**	**BIC**	**AIC**	**BIC**
30%	**378.3470**	**384.0196**	448.8439	451.6801	440.1081	445.7806	422.7788	428.4514
40%	**427.1988**	**432.8713**	479.2421	482.0784	467.4146	473.0871	456.4506	462.1232
80%	**523.5695**	**529.2421**	566.2442	569.0804	567.8633	573.5359	563.6686	569.3412
$M \mid s = 100$	**AIC**	**BIC**	**AIC**	**BIC**	**AIC**	**BIC**	**AIC**	**BIC**
30%	**295.7859**	**301.4585**	393.3030	396.1393	332.3795	338.0521	314.4786	320.1512
40%	**339.8604**	**345.5330**	417.4258	420.2621	385.4940	391.1666	367.3338	373.0064
80%	**428.0316**	**433.7042**	482.4938	485.3300	470.4306	476.1032	457.6903	463.3629

The best parametric model is chosen by means of the AIC and BIC criteria. The smallest AIC and BIC values are in bold

Table 25 Selection of the best parametric model as a function of s and M for the measure T_c^s computed on Netflix simulated data

Model selection for T_c^s-simulated data for Netflix								
	Lognormal		**Exponential**		**Weibull**		**Gamma**	
$M \mid s = 0$	**AIC**	**BIC**	**AIC**	**BIC**	**AIC**	**BIC**	**AIC**	**BIC**
30%	**367.2830**	**372.9556**	441.3489	444.1852	436.8949	442.5675	421.2143	426.8869
40%	**401.8642**	**407.5368**	469.2275	472.0638	465.7872	471.4598	452.2342	457.9068
80%	**509.6764**	**515.3490**	550.7132	553.5495	550.9566	556.6292	545.5268	551.1994
$M \mid s = 5$	**AIC**	**BIC**	**AIC**	**BIC**	**AIC**	**BIC**	**AIC**	**BIC**
30%	**350.0144**	**355.6870**	429.6711	432.5074	421.6078	427.2804	402.4658	408.1383
40%	**395.3602**	**401.0327**	461.4465	464.2828	455.0238	460.6963	440.4615	446.1340
80%	**496.7831**	**502.4557**	538.7259	541.5622	538.8420	544.5146	532.8590	538.5315
$M \mid s = 50$	**AIC**	**BIC**	**AIC**	**BIC**	**AIC**	**BIC**	**AIC**	**BIC**
30%	**280.9422**	**286.6148**	381.5252	384.3615	359.7485	365.4211	331.6124	337.2850
40%	**314.8692**	**320.5418**	401.2318	404.0681	382.8714	388.5440	360.3018	365.9744
80%	**363.5170**	**369.1895**	434.6028	437.4391	426.7378	432.4104	410.6921	416.3647
$M \mid s = 100$	**AIC**	**BIC**	**AIC**	**BIC**	**AIC**	**BIC**	**AIC**	**BIC**
30%	**254.6788**	**260.3514**	367.9003	370.7365	345.4716	351.1441	311.1198	316.7924
40%	**301.1360**	**306.8085**	393.3030	396.1393	378.2003	383.8729	353.7495	359.4221
80%	**342.3438**	**348.0164**	419.5084	422.3447	404.1885	409.8611	384.4979	390.1704

The best parametric model is chosen by means of the AIC and BIC criteria. The smallest AIC and BIC values are in bold

Table 26 Selection of the best parametric model as a function of s and M for the measure T_c^s computed on Apple simulated data

Model selection for T_c^s-simulated data for Apple								
	Lognormal		**Exponential**		**Weibull**		**Gamma**	
$M \mid s = 0$	**AIC**	**BIC**	**AIC**	**BIC**	**AIC**	**BIC**	**AIC**	**BIC**
30%	**386.5363**	**392.2088**	450.6833	453.5196	434.6305	440.3031	419.5173	425.1898
40%	**415.2923**	**420.9649**	473.4487	476.2850	449.3003	454.9729	436.1147	441.7873
80%	**526.7210**	**532.3935**	564.5002	567.3365	562.0952	567.7678	555.0535	560.7261
$M \mid s = 5$	**AIC**	**BIC**	**AIC**	**BIC**	**AIC**	**BIC**	**AIC**	**BIC**
30%	**323.6672**	**329.3398**	411.0725	413.9088	376.8005	382.4781	354.3558	360.0284
40%	**498.5114**	**504.1840**	551.9424	554.7787	553.6295	559.3021	547.8367	553.5093
80%	**571.3338**	**577.0064**	604.8417	607.6780	603.8852	609.5577	598.2251	603.8976
$M \mid s = 50$	**AIC**	**BIC**	**AIC**	**BIC**	**AIC**	**BIC**	**AIC**	**BIC**
30%	**296.4357**	**2302.1083**	392.2497	394.9860	340.7143	346.3868	320.0435	325.7161
40%	**434.3274**	**440.0000**	488.0851	490.9214	482.0709	487.7435	470.4413	476.1139
80%	**496.8472**	**502.5198**	543.8429	546.6791	545.2509	550.9234	540.0761	545.7487
$M \mid s = 100$	**AIC**	**BIC**	**AIC**	**BIC**	**AIC**	**BIC**	**AIC**	**BIC**
30%	**321.8317**	**327.5043**	404.5549	407.3912	371.8132	377.4858	352.2819	357.9545
40%	**395.5809**	**401.2534**	458.7985	461.6347	445.0042	450.6768	429.8998	435.5724
80%	**450.1114**	**455.7839**	501.9179	504.7541	502.3582	508.0308	495.7474	501.4200

The best parametric model is chosen by means of the AIC and BIC criteria. The smallest AIC and BIC values are in bold

Table 27 Selection of the best parametric model as a function of s, M and M' for the measure R_t^s computed on Tesla real data

Model selection for R_t^s-TESLA								
M=80%	**Lognormal**		**Exponential**		**Weibull**		**Gamma**	
$M' \mid s = 0$	**AIC**	**BIC**	**AIC**	**BIC**	**AIC**	**BIC**	**AIC**	**BIC**
30%	**968.4571**	**974.1297**	1.3255e+03	1.3283e+03	1.0257e+03	1.0314e+03	1.2265e+03	1.2321e+03
40%	**961.4206**	**967.0932**	1.3066e+03	1.3094e+03	1.0210e+03	1.0266e+03	1.1957e+03	1.2013e+03
50%	**953.4446**	**959.1172**	1.2808e+03	1.2837e+03	1.0141e+03	1.0198e+03	1.1629e+03	1.1686e+03
$M' \mid s = 5$	**AIC**	**BIC**	**AIC**	**BIC**	**AIC**	**BIC**	**AIC**	**BIC**
30%	**908.0326**	**913.7051**	1.1049e+03	1.1077e+03	966.0127	971.6852	1.0193e+03	1.0250e+03
40%	**755.3122**	**760.9848**	914.8652	917.7014	821.3134	826.9860	860.7029	866.3754
50%	**556.7761**	**562.4487**	597.7853	600.6216	599.6405	605.3131	595.7123	601.3849
$M' \mid s = 50$	**AIC**	**BIC**	**AIC**	**BIC**	**AIC**	**BIC**	**AIC**	**BIC**
30%	**1.0151e+03**	**1.0207e+03**	1.1641e+03	1.1670e+03	1.0616e+03	1.0673e+03	1.1029e+03	1.1086e+03
40%	**853.4507**	**859.1232**	937.7585	940.5948	901.5702	907.2427	922.1287	927.8013
50%	**755.0705**	**760.7431**	850.5152	853.3514	810.9556	816.6281	834.4726	840.1451
$M' \mid s = 100$	**AIC**	**BIC**	**AIC**	**BIC**	**AIC**	**BIC**	**AIC**	**BIC**
30%	**1.0123e+03**	**1.0180e+03**	1.1566e+03	1.1595e+03	1.0532e+03	1.0589e+03	1.0922e+03	1.0978e+03
40%	**884.1675**	**889.8401**	1.0507e+03	1.0536e+03	938.8802	944.5527	988.0512	993.7237
50%	**829.3097**	**834.9822**	1.0277e+03	1.0265e+03	889.5327	895.2053	945.6704	951.3430

The best parametric model is chosen by means of the AIC and BIC criteria. The smallest AIC and BIC values are in bold

Table 28 Selection of the best parametric model as a function of s, M and M' for the measure R_t^s computed on Netflix real data

Model selection for R_t^s-NETFLIX								
M=80%	Lognormal		Exponential		Weibull		Gamma	
M' | $s = 0$	AIC	BIC	AIC	BIC	AIC	BIC	AIC	BIC
30%	**1.0361e+03**	**1.0418e+03**	1.3764e+03	1.3792e+03	1.0778e+03	1.0834e+03	1.2958e+03	1.3015e+03
40%	**1.0380e+03**	**1.0437e+03**	1.3744e+03	1.3772e+03	1.0802e+03	1.0959e+03	1.2843e+03	1.2900e+03
50%	**1.0323e+03**	**1.0380e+03**	1.3702e+03	1.3730e+03	1.0753e+03	1.0809e+03	1.2800e+03	1.2856e+03
M' | $s = 5$	AIC	BIC	AIC	BIC	AIC	BIC	AIC	BIC
30%	**1.0783e+03**	**1.0839e+03**	1.2926e+03	1.2955e+03	1.1236e+03	1.1293e+03	1.1915e+03	1.1972e+03
40%	**989.0394**	**994.7120**	1.2154e+03	1.2183e+03	1.0407e+03	1.0463e+03	1.1026e+03	1.1083e+03
50%	**868.0608**	**873.7333**	1.1150e+03	1.1178e+03	933.0974	938.7699	993.1070	998.7796
M' | $s = 50$	AIC	BIC	AIC	BIC	AIC	BIC	AIC	BIC
30%	**1.0509e+03**	**1.0566e+03**	1.2530e+03	1.2558e+03	1.1014e+03	1.1071e+03	1.0576+03	1.0633e+03
40%	**967.5316**	**973.2041**	1.2033e+03	1.2061e+03	1.0295e+03	1.0351e+03	1.1093e+03	1.1150e+03
50%	**905.9353**	**911.6079**	1.1770e+03	1.1799e+03	971.1089	976.7815	1.1713e+03	1.1770e+03
M' | $s = 100$	AIC	BIC	AIC	BIC	AIC	BIC	AIC	BIC
30%	**960.0611**	**965.7337**	1.2244e+03	1.2272e+03	1.0199e+03	1.0255e+03	1.1135e+03	1.1191e+03
40%	**921.6886**	**927.3612**	1.1855e+03	1.1883e+03	982.9280	988.6005	1.0662e+03	1.0719e+03
50%	**849.4650**	**855.1376**	1.1589e+03	1.1618e+03	917.0612	922.7337	1.0087e+03	1.0143e+03

The best parametric model is chosen by means of the AIC and BIC criteria. The smallest AIC and BIC values are in bold

Table 29 Selection of the best parametric model as a function of s, M and M' for the measure R_t^s computed on Apple real data

Model selection for R_t^s-APPLE								
M=80%	Lognormal		Exponential		Weibull		Gamma	
M' | $s = 0$	AIC	BIC	AIC	BIC	AIC	BIC	AIC	BIC
30%	**1.0024e+03**	**1.0081e+03**	1.3678e+03	1.3706e+03	1.0518e+03	1.0574e+03	1.2893e+03	1.2949e+03
40%	**995.3318**	**1.0010e+03**	1.3678e+03	1.3706e+03	1.0466e+03	1.0523e+03	1.2712e+03	1.2768e+03
50%	**977.2639**	**982.9365**	1.3621e+03	1.3649e+03	1.0309e+03	1.0366e+03	1.2577e+03	1.2634e+03
M' | $s = 5$	AIC	BIC	AIC	BIC	AIC	BIC	AIC	BIC
30%	**1.0632e+03**	**1.0688e+03**	1.2149e+03	1.2177e+03	1.1092e+03	1.1149e+03	1.1487e+03	1.1544e+03
40%	**907.9526**	**913.6251**	1.0962e+03	1.0991e+03	972.3222	977.9948	1.1255e+03	1.0312e+03
50%	**736.9171**	**742.5897**	964.0400	966.8763	825.9198	831.5924	896.9408	902.6134
M' | $s = 50$	AIC	BIC	AIC	BIC	AIC	BIC	AIC	BIC
30%	**966.2662**	**971.9387**	1.0456e+03	1.0485e+03	1.0023e+03	1.0079e+03	1.0194+03	1.0251e+03
40%	**888.8694**	**894.5419**	974.2439	977.0802	931.9785	937.6511	951.6929	957.3654
50%	**763.3344**	**769.0069**	818.7865	821.6228	804.0412	809.7137	814.9187	820.5912
M' | $s = 100$	AIC	BIC	AIC	BIC	AIC	BIC	AIC	BIC
30%	**1.0526e+03**	**1.0583e+03**	1.1999e+03	1.2028e+03	1.0952e+03	1.1008e+03	1.1468e+03	1.1525e+03
40%	**946.6623**	**952.3348**	1.1337e+03	1.1365e+03	1.0009e+03	1.0066e+03	1.0645e+03	1.0702e+03
50%	**864.3296**	**870.0021**	1.0934e+03	1.0963e+03	928.3033	933.9758	1.0019e+03	1.0076e+03

The best parametric model is chosen by means of the AIC and BIC criteria. The smallest AIC and BIC values are in bold

Table 30 Selection of the best parametric model as a function of s, M and M' for the measure R_t^s computed on Tesla simulated data

Model selection for R_t^s-simulated data for TESLA								
M=80%	Lognormal		Exponential		Weibull		Gamma	
M' | $s=0$	AIC	BIC	AIC	BIC	AIC	BIC	AIC	BIC
30%	**1.0326e+03**	**1.0383e+03**	1.3185e+03	1.3214e+03	1.0730e+03	1.0787e+03	1.5154e+03	1.5210e+03
40%	**1.0634e+03**	**1.0690e+03**	1.3352e+03	1.3380e+03	1.1154e+03	1.1211e+03	1.2925e+03	1.2982e+03
50%	**997.1760**	**1.0028e+03**	1.2604e+03	1.2632e+03	1.0555e+03	1.0611e+03	1.1729e+03	1.1786e+03
M' | $s=5$	AIC	BIC	AIC	BIC	AIC	BIC	AIC	BIC
30%	**1.0840e+03**	**1.0897e+03**	1.3582e+03	1.3611e+03	1.1325e+03	1.1382e+03	1.3766e+03	1.3823e+03
40%	**1.0345e+03**	**1.0402e+03**	1.2439e+03	1.2467e+03	1.0905e+03	1.0962e+03	1.0703e+03	1.1766e+03
50%	**939.9660**	**945.6386**	1.1266e+03	1.1294e+03	999.8915	1.0056e+03	1.0646e+03	1.1823e+03
M' | $s=50$	AIC	BIC	AIC	BIC	AIC	BIC	AIC	BIC
30%	**1.0867e+03**	**1.0924e+03**	1.2871e+03	1.2899e+03	1.1375e+03	1.1057e+03	1.2239e+03	1.2296e+03
40%	**1.0041e+03**	**1.0098e+03**	1.1697e+03	1.1725e+03	1.0500e+03	1.0557e+03	1.1065e+03	1.1121e+03
50%	**868.0009**	**873.6735**	1.0243e+03	1.0271e+03	920.6579	926.3305	976.1139	926.4127
M' | $s=100$	AIC	BIC	AIC	BIC	AIC	BIC	AIC	BIC
30%	**1.0137e+03**	**1.0194e+03**	1.0684e+03	1.0713e+03	1.0387e+03	1.0443e+03	1.0493e+03	1.0550e+03
40%	**940.5239**	**946.1965**	988.8454	991.6817	965.8764	971.5490	976.0319	981.7045
50%	**864.1064**	**869.7789**	909.7296	912.5659	891.8050	897.4770	901.3648	907.0373

The best parametric model is chosen by means of the AIC and BIC criteria. The smallest AIC and BIC values are in bold

To apply our findings, we conduct a simple practical example, using Tesla stock. First, we set $s = 5$, followed by $s = 50$, and then assess our risk measures using their parametric distributions. Concerning the time to crash T_c^s, in the first scenario, when $s = 5$, there is approximately an 81

Now, we extend the example to the recovery time R_t^s and speed of recovery S_r^s, always using $s = 5$ and $s = 50$, and setting $M = 80\%$ and $M' = 30\%$. For R_t^s, at $s = 5$, the probability of having a drawdown change of M intensity and, immediately after, a new variation equal to M' within the first five minutes of the trading day is 43%. Furthermore, the probability that these drawdown variations occur with a speed S_r^s less than 0.5 min^{-1} is equal to 89.6%. For the second scenario, when $s = 50$, the likelihood of first experiencing a M drawdown variation and then a M' change during the first five minutes is equal to 34%. In addition, these changes will happen with a speed less than 0.5 min^{-1}, with a probability equal to 93.4%.

Figure 3 shows the results of the example just stated for $s = 5$ and $s = 50$. The first part of the graph shows the cumulative probability distributions for the first 20 min of the trading day for the time to crash and the speed of crash, considering the $M = 30\%$ threshold. Considering this, the cumulative probability distributions of the time to crash and the speed of crash provide information on the likelihood of crossing the 30% threshold, and how rapidly this occurs, minute by minute. Specifically, the second portion of the graph shows the cumulative probability distributions for both the recovery time and the speed of recovery during the initial 20 min of the trading day, with $M = 80\%$ and

Table 31 Selection of the best parametric model as a function of s, M and M' for the measure R_t^s computed on Netflix simulated data

Model selection for R_t^s-simulated data for NETFLIX								
M=80%	Lognormal		Exponential		Weibull		Gamma	
$M' \mid s=0$	AIC	BIC	AIC	BIC	AIC	BIC	AIC	BIC
30%	**1.1309e+03**	**1.1366e+03**	1.3318e+03	1.3346e+03	1.1715e+03	1.1772e+03	1.2732e+03	1.2789e+03
40%	**1.0610e+03**	**1.0667e+03**	1.2630e+03	1.2959e+03	1.1055e+03	1.1112e+03	1.1870e+03	1.1926e+03
50%	**978.2024**	**983.8749**	1.1597e+03	1.1626e+03	1.0236e+03	1.0293e+03	1.0825e+03	1.0882e+03
$M' \mid s=5$	AIC	BIC	AIC	BIC	AIC	BIC	AIC	BIC
30%	**1.0959e+03**	**1.1016e+03**	1.3214e+03	1.3242e+03	1.1465e+03	1.1522e+03	1.2793e+03	1.2850e+03
40%	**1.0309e+03**	**1.0366e+03**	1.2723e+03	1.2751e+03	1.0858e+03	1.0915e+03	1.1989e+03	1.2046e+03
50%	**1.0059e+03**	**1.0115e+03**	1.2075e+03	1.2104e+03	1.0550e+03	1.0607e+03	1.1276e+03	1.1332e+03
$M' \mid s=50$	AIC	BIC	AIC	BIC	AIC	BIC	AIC	BIC
30%	**1.0231e+03**	**1.0287+03**	1.1597e+03	1.1625e+03	1.0626e+03	1.0683e+03	1.1151e+03	1.1208e+03
40%	**982.4874**	**988.1599**	1.1393e+03	1.1421e+03	1.0278e+03	1.0334e+03	1.0854e+03	1.0911e+03
50%	**943.4720**	**949.1446**	1.0674e+03	1.0703e+03	983.4023	989.0749	1.0241e+03	1.0298e+03
$M' \mid s=100$	AIC	BIC	AIC	BIC	AIC	BIC	AIC	BIC
30%	**902.1937**	**907.8862**	1.0443e+03	1.0472e+03	948.8200	954.4925	993.3576	999.0302
40%	**860.9473**	**866.6199**	1.0128e+03	1.0157e+03	913.0693	918.7419	961.4471	967.1197
50%	**817.5565**	**823.2290**	895.3954	898.2317	855.7938	861.4664	873.7375	879.4100

The best parametric model is chosen by means of the AIC and BIC criteria. The smallest AIC and BIC values are in bold

$M' = 30\%$. Consequently, these cumulative probability distributions provide insights into the likelihood of surpassing the 30% threshold after surpassing the 80% threshold, as well as the rate at which this happens per minute.

Conclusion

In this study, we examine various risk indicators related to market crises for high-frequency financial volumes of assets listed on the Nasdaq Stock Exchange, such as Tesla, Netflix, and Apple. We introduce a commencement time s to calculate the drawdown-based risk indicators in daily intervals, thereby preventing our risk indicators from being affected by the initial large volume of transactions. We generate artificial time series of volumes using the WISMC model, a variant of the conventional semi-Markov chain model. Next, we compute all drawdown-based risk measures on both actual and simulated data, and investigate them using parametric models. The estimation procedures for these models consider the right censorship. Lastly, we measure the distance between real and simulated risk measures using the Kullback–Leibler divergence. Overall, our findings are financially significant, because they offer insight into an asset"s liquidity risk, and therefore, can be used for financial investments.

Table 32 Selection of the best parametric model as a function of s, M and M' for the measure R_t^s computed on APPLE simulated data

Model selection for R_t^s-simulated data for APPLE								
M=80%	**Lognormal**		**Exponential**		**Weibull**		**Gamma**	
M' | $s = 0$	**AIC**	**BIC**	**AIC**	**BIC**	**AIC**	**BIC**	**AIC**	**BIC**
30%	**1.1635e+03**	**1.692e+03**	1.3839e+03	1.3868e+03	1.2043e+03	1.2099e+03	1.3705e+03	1.3762e+03
40%	**1.0663e+03**	**1.0719e+03**	1.2982e+03	1.3010e+03	1.1181e+03	1.1237e+03	1.2279e+03	1.2336e+03
50%	**952.0155**	**957.6881**	1.0814e+03	1.0842e+03	996.7772	1.0024e+03	1.0383e+03	1.0440e+03
M' | $s = 5$	**AIC**	**BIC**	**AIC**	**BIC**	**AIC**	**BIC**	**AIC**	**BIC**
30%	**1.1715e+03**	**1.0682e+03**	1.3693e+03	1.3722e+03	1.2146e+03	1.2203e+03	1.3535e+03	1.3592e+03
40%	**1.0682e+03**	**1.0739e+03**	1.2301e+03	1.2329e+03	1.1145e+03	1.1201e+03	993.4517	999.1242
50%	**957.2985**	**962.9711**	1.0039e+03	1.0067e+03	982.4105	988.0830	993.4517	999.1242
M' | $s = 50$	**AIC**	**BIC**	**AIC**	**BIC**	**AIC**	**BIC**	**AIC**	**BIC**
30%	**1.0515e+03**	**1.0572e+03**	1.1927+03	1.1956+03	1.1000+03	1.1057e+03	1.1523e+03	1.1580e+03
40%	**955.5430**	**961.2155**	1.0827+03	1.0855+03	1.0091+03	1.0147+03	1.0509+03	1.0566+03
50%	**852.3765**	**858.0491**	933.0831	935.9094	901.2634	906.9360	920.7401	926.4127
M' | $s = 100$	**AIC**	**BIC**	**AIC**	**BIC**	**AIC**	**BIC**	**AIC**	**BIC**
30%	**1.0343e+03**	**1.0400e+03**	1.1503e+03	1.1531e+03	1.0686e+03	1.0743e+03	1.1031e+03	1.1087e+03
40%	**957.3771**	**963.0496**	1.0217e+03	1.0245e+03	985.0520	990.7245	998.5607	1.0042e+03
50%	**868.0799**	**873.7524**	933.0373	935.9094	900.6337	906.3062	914.7511	920.4237

The best parametric model is chosen by means of the AIC and BIC criteria. The smallest AIC and BIC values are in bold

Table 33 Parameters of the best parametric models for T_c^s computed on real and simulated data for Tesla

Summary of the best statistical model selection				
for T_c^s-TESLA				
$s = 0$	M	Best model	Real data (μ, σ)	Simulated data (μ, σ)
	30%	Lognormal	0.0877–0.3399	0.5806–0.6975
	40%	Lognormal	0.1129–0.3733	0.7110–0.8040
	80%	Lognormal	0.1384–0.4066	0.9193–0.9602
$s = 5$	**M**	**Best model**	**Real data (μ, σ)**	**Simulated data (μ, σ)**
	30%	Lognormal	0.9041–0.8164	0.6380–0.7215
	40%	Lognormal	1.2313–0.9856	0.7868–0.8303
	80%	Lognormal	1.4796–1.0228	0.9973–0.9272
$s = 50$	**M**	**Best model**	**Real data (μ, σ)**	**Simulated data (μ, σ)**
	30%	Lognormal	0.3989–0.5211	0.4982–0.6520
	40%	Lognormal	0.5723–0.6550	0.6047–0.7115
	80%	Lognormal	0.7741–0.7735	0.8020–0.8563
$s = 100$	**M**	**Best model**	**Real data (μ, σ)**	**Simulated data (μ, σ)**
	30%	Lognormal	0.1857–0.3694	0.4075–0.5145
	40%	Lognormal	0.3282–0.4584	0.4483–0.5883
	80%	Lognormal	0.4978–0.5804	0.6265–0.6985

Table 34 Parameters of the best parametric models for T_c^s computed on real and simulated data for Netflix

Summary of the best statistical model selection				
for T_c^s-NETFLIX				
$s = 0$	***M***	**Best model**	**Real data (μ, σ)**	**Simulated data (μ, σ)**
	30%	Lognormal	0.1004–0.5073	0.4419–0.6602
	40%	Lognormal	0.1113–0.5535	0.5362–0.6892
	80%	Lognormal	0.1222–0.6969	0.7718–0.8352
$s = 5$	***M***	**Best Model**	**Real data (μ, σ)**	**Simulated data (μ, σ)**
	30%	Lognormal	0.7698–0.8593	0.4267–0.6259
	40%	Lognormal	1.2313–0.9856	0.5257–0.6786
	80%	Lognormal	1.0192–1.0803	0.7312–0.8264
$s = 50$	***M***	**Best Model**	**Real data (μ, σ)**	**Simulated data (μ, σ)**
	30%	Lognormal	0.3247–0.6870	0.3054–0.5372
	40%	Lognormal	0.4590–0.7731	0.3600–0.5819
	80%	Lognormal	0.5667–0.9256	0.4326–0.6565
$s = 100$	***M***	**Best Model**	**Real data (μ, σ)**	**Simulated data (μ, σ)**
	30%	Lognormal	0.2669–0.5030	0.5806–0.6975
	40%	Lognormal	0.3975–0.6388	0.3246–0.5710
	80%	Lognormal	0.4937–0.8195	0.4144–0.6146

Table 35 Parameters of the best parametric models for T_c^s computed on real and simulated data for Apple

Summary of the best statistical model selection				
for T_c^s-APPLE				
$s = 0$	***M***	**Best model**	**Real data (μ, σ)**	**Simulated data (μ, σ)**
	30%	Lognormal	0.0330–0.1482	0.5250–0.6557
	40%	Lognormal	0.0495–0.2349	0.6359–0.6579
	80%	Lognormal	0.0770–0.3069	0.8650–0.8141
$s = 5$	***M***	**Best model**	**Real data (μ, σ)**	**Simulated data (μ, σ)**
	30%	Lognormal	0.5917–0.6636	0.4381–0.5573
	40%	Lognormal	0.8012–0.7931	0.7647–0.8047
	80%	Lognormal	0.9900–0.8993	1.0009–0.8483
$s = 50$	***M***	**Best model**	**Real data (μ, σ)**	**Simulated data (μ, σ)**
	30%	Lognormal	0.3130–0.4504	0.3922–0.5238
	40%	Lognormal	0.5157–0.6311	0.6145–0.7248
	80%	Lognormal	0.8013–0.7750	0.7285–0.8288
$s = 100$	***M***	**Best model**	**Real data (μ, σ)**	**Simulated data (μ, σ)**
	30%	Lognormal	0.3517-0.4951	0.4024–0.5734
	40%	Lognormal	0.4972–0.5911	0.5489–0.6637
	80%	Lognormal	0.6628–0.7115	0.5882–0.7923

Table 36 Parameters of the best models for R_t^s computed on real and simulated data for Tesla

Summary of the best statistical model selection				
for R_t^s-TESLA fixing $M = 80\%$				
$s = 0$	M'	**Best model**	**Real data (μ, σ)**	**Simulated data (μ, σ)**
	30%	Lognormal	2.4518–2.1359	3.8690–2.6808
	40%	Lognormal	2.3364–2.0065	2.8326–1.9657
	50%	Lognormal	2.2232–1.8870	2.3551–1.7134
$s = 5$	M'	**Best model**	**Real data (μ, σ)**	**Simulated data (μ, σ)**
	30%	Lognormal	1.8449–1.4644	3.1969–2.1557
	40%	Lognormal	1.3389–1.2555	2.4572–1.5758
	50%	Lognormal	0.9199–0.8682	2.0759–1.3965
$s = 50$	M'	**Best model**	**Real data (μ, σ)**	**Simulated data (μ, σ)**
	30%	Lognormal	2.2509–1.4937	2.6348–1.7452
	40%	Lognormal	1.7833–1.1883	2.2369–1.5401
	50%	Lognormal	1.4324–1.1423	1.7545–1.3654
$s = 100$	M'	**Best model**	**Real data (μ, σ)**	**Simulated data (μ, σ)**
	30%	Lognormal	2.1978–1.5592	2.2634–1.3890
	40%	Lognormal	1.7927–1.4021	2.0196–1.3255
	50%	Lognormal	1.5762–1.3999	1.7640–1.2639

Table 37 Parameters of the best models for R_t^s computed on real and simulated data for Netflix

Summary of the best statistical model selection				
for R_t^s-NETFLIX fixing $M = 80\%$				
$s = 0$	M'	**Best model**	**Real data (μ, σ)**	**Simulated data (μ, σ)**
	30%	Lognormal	2.7483–2.5359	2.8195–1.8600
	40%	Lognormal	2.6975–2.4817	2.4759–1.7315
	50%	Lognormal	2.4494–1.7925	2.1006–1.5940
$s = 5$	M'	**Best model**	**Real data (μ, σ)**	**Simulated data (μ, σ)**
	30%	Lognormal	2.0871–1.6907	2.8411–1.7920
	40%	Lognormal	1.3389–1.2555	2.4902–1.7140
	50%	Lognormal	1.6473–1.5233	2.2511–1.6284
$s = 50$	M'	**Best model**	**Real data (μ, σ)**	**Simulated data (μ, σ)**
	30%	Lognormal	2.4181–1.6505	2.3354–1.5037
	40%	Lognormal	2.1419–1.5548	2.1854–1.4858
	50%	Lognormal	1.8792–1.5830	2.0071–1.4330
$s = 100$	M'	**Best model**	**Real data (μ, σ)**	**Simulated data (μ, σ)**
	30%	Lognormal	2.1027–1.6756	1.8558–1.4143
	40%	Lognormal	1.9135–1.6314	1.7284–1.3628
	50%	Lognormal	1.6221–1.6373	1.5494–1.3021

Table 38 Parameters of the best models for R_t^s computed on real and simulated data for Apple

Summary of the best statistical model selection				
for R_t^s-APPLE fixing $M = 80\%$				
$s = 0$	M'	**Best model**	**Real data (μ, σ)**	**Simulated data (μ, σ)**
	30%	Lognormal	2.7049–2.4575	3.2072–2.0500
	40%	Lognormal	2.6150–2.4137	2.6112–1.7552
	50%	Lognormal	2.5477–2.3907	2.0644–1.3993
$s = 5$	M'	**Best model**	**Real data (μ, σ)**	**Simulated data (μ, σ)**
	30%	Lognormal	2.4150–1.5356	3.1767–1.8703
	40%	Lognormal	1.9141–1.3644	2.5502–1.5439
	50%	Lognormal	1.4178–1.1321	2.1096–1.2948
$s = 50$	M'	**Best model**	**Real data (μ, σ)**	**Simulated data (μ, σ)**
	30%	Lognormal	2.0998–1.3549	2.4960–1.4318
	40%	Lognormal	1.8531–1.2754	2.1636–1.2831
	50%	Lognormal	1.4735–1.1329	1.8042–1.1588
$s = 100$	M'	**Best model**	**Real data (μ, σ)**	**Simulated data (μ, σ)**
	30%	Lognormal	2.4287–1.5425	2.3031–1.5313
	40%	Lognormal	2.0531–1.4699	2.0355–1.3949
	50%	Lognormal	1.7431–1.4430	1.7345–1.3223

Table 39 Descriptive statistics of T_c^s (first quartile, second quartile (median), third quartile, mean, standard deviation, asymmetry index) and related censored units as a function of M and s

Descriptive statistics of T_c^s-TESLA							
$s = 0$ (%)	**Q1**	**Q2**	**Q3**	**Mean**	**SD**	**AI**	**Censoring rate (%)**
$M = 30$	0.8680	1.0917	1.3729	1.1566	0.4048	0.4812	0
$M = 40$	0.8703	1.1195	1.4401	1.2003	0.4641	0.5222	0
$M = 80$	0.8730	1.11484	1.5108	1.2474	0.5289	0.5614	0
$s = 5$ (%)	**Q1**	**Q2**	**Q3**	**Mean**	**SD**	**AI**	**Censoring rate (%)**
$M = 30$	1.4240	2.4697	4.2834	3.4465	3.3547	0.8735	0
$M = 40$	1.7621	3.4257	6.6597	5.5678	7.1339	0.9008	0
$M = 80$	2.2028	4.3912	8.7536	7.4087	10.0677	0.8992	0
$s = 50$ (%)	**Q1**	**Q2**	**Q3**	**Mean**	**SD**	**AI**	**Censoring rate (%)**
$M = 30$	1.0486	1.4902	2.1178	1.7069	0.9534	0.6819	0
$M = 40$	1.1394	1.7723	2.7569	2.1964	1.6077	0.7913	0
$M = 80$	1.2871	2.1686	3.6540	2.9249	2.6470	0.8571	0
$s = 100$ (%)	**Q1**	**Q2**	**Q3**	**Mean**	**SD**	**AI**	**Censoring rate (%)**
$M = 30$	0.9385	1.2041	1.5447	1.2891	0.4929	0.5175	0
$M = 40$	1.0192	1.3885	1.8915	1.5423	0.7458	0.6187	0
$M = 80$	1.1122	1.6451	2.4334	1.9469	1.2322	0.7348	0

Table 40 Descriptive statistics of T_c^s (first quartile, second quartile (median), third quartile, mean, standard deviation, asymmetry index) and related censored units as a function of M and s

Descriptive statistics of T_c^s-NETFLIX							
$s = 0$ (%)	**Q1**	**Q2**	**Q3**	**Mean**	**SD**	**AI**	**Censoring rate (%)**
$M = 30$	0.7852	1.1056	1.5567	1.2574	0.6812	0.6686	0
$M = 40$	0.7695	1.1177	1.6236	1.3028	0.7800	0.7116	0
$M = 80$	0.7062	1.1300	1.8081	1.4406	1.1391	0.8180	0.8
$s = 5$ (%)	**Q1**	**Q2**	**Q3**	**Mean**	**SD**	**AI**	**Censoring rate (%)**
$M = 30$	1.0337	1.8152	3.1876	2.5719	2.5815	0.8794	0
$M = 40$	1.2095	2.1593	3.8551	3.1236	3.2650	0.8860	0
$M = 80$	1.3372	2.7710	5.7423	4.9665	7.3875	0.8916	0.8
$s = 50$ (%)	**Q1**	**Q2**	**Q3**	**Mean**	**SD**	**AI**	**Censoring rate (%)**
$M = 30$	0.8705	1.3836	2.1992	1.7519	1.3605	0.8120	0
$M = 40$	0.9395	1.5825	2.6657	2.1337	1.9296	0.8569	0
$M = 80$	0.9440	1.7624	3.9204	2.7049	3.1492	0.8978	1.6
$s = 100$ (%)	**Q1**	**Q2**	**Q3**	**Mean**	**SD**	**AI**	**Censoring rate (%)**
$M = 30$	0.9075	1.3197	1.9190	1.5395	0.9248	0.7131	0
$M = 40$	0.9672	1.4881	2.2896	1.8249	1.2954	0.7800	0
$M = 80$	0.9427	1.6384	2.8475	2.2921	2.2427	0.8745	1.6

Table 41 Descriptive statistics of T_c^s (first quartile, second quartile (median), third quartile, mean, standard deviation, asymmetry index) and related censored units as a function of M and s

Descriptive statistics of T_c^s-APPLE							
$s = 0$ (%)	**Q1**	**Q2**	**Q3**	**Mean**	**SD**	**AI**	**Censoring rate (%)**
$M = 30$	0.9352	1.0336	1.1422	1.0450	0.1557	0.2199	0
$M = 40$	0.8968	1.0507	1.2311	1.0801	0.2573	0.3428	0
$M = 80$	0.8783	1.0800	1.3281	1.1320	0.3553	0.4386	0
$s = 5$ (%)	**Q1**	**Q2**	**Q3**	**Mean**	**SD**	**AI**	**Censoring rate (%)**
$M = 30$	1.1550	1.8071	2.8272	2.2521	1.6752	0.7971	0
$M = 40$	1.3051	2.2282	3.8043	3.0517	2.8558	0.8942	0
$M = 80$	1.4673	2.6912	4.9361	4.0324	4.4995	0.8577	0
$s = 50$ (%)	**Q1**	**Q2**	**Q3**	**Mean**	**SD**	**AI**	**Censoring rate (%)**
$M = 30$	1.0093	1.3675	1.8530	1.5135	0.7178	0.6102	0
$M = 40$	1.0942	1.6748	2.5635	2.0439	1.4296	0.7744	0
$M = 80$	1.3212	2.2284	3.7585	3.0090	2.7302	0.8577	0
$s = 100$ (%)	**Q1**	**Q2**	**Q3**	**Mean**	**SD**	**AI**	**Censoring rate (%)**
$M = 30$	1.0179	1.4215	1.9850	1.6068	0.8469	0.6566	0
$M = 40$	1.1035	1.6441	2.4495	1.9580	1.2662	0.7436	0
$M = 80$	1.2007	1.9402	3.1352	2.4991	2.0288	0.8264	0

Table 42 Descriptive statistics of S_c^s (First Quartile, Second Quartile (Median), Third Quartile, Mean, Standard Deviation, Asymmetry Index) and related censored units as a function of M and s

Descriptive statistics of S_c^s-TESLA							
$s = 0$ (%)	Q1	Q2	Q3	Mean	SD	AI	Censoring rate (%)
$M = 30$	0.1250	0.2250	0.2250	0.1097	0.1027	−3.3693	0
$M = 40\%$	0.1667	0.3000	0.3000	0.1464	0.1305	−3.5311	0
$M = 80$	0.3333	0.3333	0.6000	0.2949	0.2489	−0.4632	0
$s = 5$ (%)	Q1	Q2	Q3	Mean	SD	AI	Censoring rate (%)
$M = 30$	0.0550	0.0875	0.1250	0.1035	0.0648	0.7412	0
$M = 40$	0.0536	0.0900	0.1667	0.1157	0.0858	0.8990	0
$M = 80$	0.0844	0.1467	0.2333	0.2080	0.1649	1.1161	0
$s = 50$ (%)	Q1	Q2	Q3	Mean	SD	AI	Censoring rate (%)
$M = 30$	0.0875	0.1250	0.2250	0.1232	0.0707	−0.0752	0
$M = 40$	0.1167	0.1667	0.1667	0.1563	0.0889	−0.3513	0
$M = 80$	0.1800	0.2333	0.3333	0.2883	0.1749	0.9421	0
$s = 100$ (%)	Q1	Q2	Q3	Mean	SD	AI	Censoring rate (%)
$M = 30$	0.1250	0.1250	0.2250	0.1155	0.0919	−0.3117	0
$M = 40$	0.1667	0.1667	0.3000	0.1645	0.1003	−0.0659	0
$M = 80$	0.2333	0.3333	0.3333	0.3258	0.1789	−0.1259	0

Table 43 Descriptive statistics of S_c^s (First Quartile, Second Quartile (Median), Third Quartile, Mean, Standard Deviation, Asymmetry Index) and related censored units as a function of M and s

Descriptive statistics of S_c^s-NETFLIX							
$s = 0$ (%)	Q1	Q2	Q3	Mean	SD	AI	Censoring rate (%)
$M = 30$	0.1250	0.1250	0.2250	0.1026	0.0901	−0.7453	0
$M = 40$	0.1667	0.1667	0.3000	0.1351	0.1166	−0.8130	0
$M = 80$	0.3333	0.3333	0.6000	0.2525	0.2205	−1.0997	0.8
$s = 5$ (%)	Q1	Q2	Q3	Mean	SD	AI	Censoring rate (%)
$M = 30$	0.0675	0.1250	0.1250	0.1028	0.0697	−0.9579	0
$M = 40$	0.0900	0.1167	0.1667	0.1356	0.0899	0.6331	0
$M = 80$	0.1238	0.2333	0.3333	0.2300	0.1804	−0.0552	0.8
$s = 50$ (%)	Q1	Q2	Q3	Mean	SD	AI	Censoring rate (%)
$M = 30$	0.0875	0.1250	0.2250	0.1065	0.0754	−0.7351	0
$M = 40$	0.1167	0.1667	0.3000	0.1398	0.0957	−0.8430	0
$M = 80$	0.1800	0.3333	0.6000	0.2560	0.1894	−1.2255	1.6
$s = 100$ (%)	Q1	Q2	Q3	Mean	SD	AI	Censoring rate (%)
$M = 30$	0.1250	0.1250	0.2250	0.1136	0.0781	−0.4391	0
$M = 40$	0.1167	0.1667	0.3000	0.1513	0.0965	−0.4779	0
$M = 80$	0.2333	0.3333	0.6000	0.2725	0.1905	−0.9584	1.6

Table 44 Descriptive statistics of S_c^s (First Quartile, Second Quartile (Median), Third Quartile, Mean, Standard Deviation, Asymmetry Index) and related censored units as a function of M and s

Descriptive statistics of S_c^s-APPLE							
$s = 0$ (%)	**Q1**	**Q2**	**Q3**	**Mean**	**SD**	**AI**	**Censoring rate (%)**
$M = 30$	0.1250	0.1250	0.2250	0.1970	0.0835	2.5859	0
$M = 40$	0.1667	0.3000	0.3000	0.1714	0.1474	−2.6175	0
$M = 80$	0.3333	0.6000	0.6000	0.2988	0.2835	−3.1872	0
$s = 5$ (%)	**Q1**	**Q2**	**Q3**	**Mean**	**SD**	**AI**	**Censoring rate (%)**
$M = 30$	0.0875	0.1250	0.1250	0.1167	0.0664	−0.3738	0
$M = 40$	0.0900	0.1167	0.1667	0.1419	0.0875	0.8644	0
$M = 80$	0.1467	0.2333	0.3333	0.2579	0.1747	0.4216	0
$s = 50$ (%)	**Q1**	**Q2**	**Q3**	**Mean**	**SD**	**AI**	**Censoring rate (%)**
$M = 30$	0.1250	0.1250	0.2250	0.1227	0.0765	−0.0891	0
$M = 40$	0.1167	0.1667	0.1667	0.1575	0.0904	−0.3043	0
$M = 80$	0.1800	0.2333	0.3333	0.2875	0.1739	0.9334	0
$s = 100$ (%)	**Q1**	**Q2**	**Q3**	**Mean**	**SD**	**AI**	**Censoring rate (%)**
$M = 30$	0.1250	0.1250	0.2250	0.1225	0.0735	−0.1012	0
$M = 40$	0.1167	0.1667	0.1667	0.1616	0.0899	−0.1691	0
$M = 80$	0.1800	0.3333	0.3333	0.3019	0.1760	−0.5352	0

Table 45 Descriptive statistics of R_t^s (First Quartile, Second Quartile (Median), Third Quartile, Mean, Standard Deviation, Asymmetry Index) and related censored units as a function of s, M and M'

Descriptive statistics of R_t^s-TESLA with $M = 80\%$							
$s = 0$ (%)	**Q1**	**Q2**	**Q3**	**Mean**	**SD**	**AI**	**Censoring rate (%)**
$M' = 30$	2.7488	11.6092	49.0305	113.6171	1.1061e+03	0.2767	9
$M' = 40$	2.6726	10.3439	40.0354	77.4336	574.4651	0.3504	8
$M' = 50$	2.5868	9.2368	32.9820	54.7942	320.3950	0.4266	6
$s = 5$ (%)	**Q1**	**Q2**	**Q3**	**Mean**	**SD**	**AI**	**Censoring rate (%)**
$M' = 30$	2.3565	6.3275	16.9900	18.4882	50.7585	0.7187	0.8
$M' = 40$	1.6357	3.8148	8.8971	8.3900	16.4344	0.8352	0
$M' = 50$	1.3970	2.5049	4.5064	3.6575	3.8794	0.8881	0
$s = 50$ (%)	**Q1**	**Q2**	**Q3**	**Mean**	**SD**	**AI**	**Censoring rate (%)**
$M' = 30$	3.4674	9.4963	26.0075	28.9761	83.5318	0.6996	0.8
$M' = 40$	2.6693	5.9495	13.2606	12.0532	21.2368	0.8622	0
$M' = 50$	1.9385	4.1887	9.0509	8.0432	13.1848	0.8770	0
$s = 100$ (%)	**Q1**	**Q2**	**Q3**	**Mean**	**SD**	**AI**	**Censoring rate (%)**
$M' = 30$	3.1460	9.0052	25.7765	30.3669	97.7956	0.6553	0.8
$M' = 40$	2.3326	6.0056	15.4623	16.0489	39.7717	0.7556	0.8
$M' = 50$	1.8813	4.8365	12.4338	12.8850	31.8165	0.7589	0.8

Table 46 Descriptive statistics of R_t^s (First Quartile, Second Quartile (Median), Third Quartile, Mean, Standard Deviation, Asymmetry Index) and related censored units as a function of *s*, *M* and *M*′

Descriptive statistics of R_t^s-NETFLIX with $M = 80\%$							
$s = 0$ (%)	**Q1**	**Q2**	**Q3**	**Mean**	**SD**	**AI**	**Censoring rate (%)**
$M' = 30$	2.8232	15.6116	86.3785	389.0448	9.6845e+03	0.1157	11
$M' = 40$	2.7832	14.8426	79.1529	322.7627	7.0113e+03	0.1318	10
$M' = 50$	2.7576	14.5778	76.7872	302.9809	6.2898e+03	0.1376	10
$s = 5$ (%)	**Q1**	**Q2**	**Q3**	**Mean**	**SD**	**AI**	**Censoring rate (%)**
$M' = 30$	3.4569	11.5814	38.8001	57.7387	282.0047	0.4910	2
$M' = 40$	2.5773	8.0615	25.2155	33.6608	136.4602	0.5628	1.6
$M' = 50$	1.8586	5.1929	14.5087	16.5688	50.2015	0.6798	0.8
$s = 50$ (%)	**Q1**	**Q2**	**Q3**	**Mean**	**SD**	**AI**	**Censoring rate (%)**
$M' = 30$	3.6872	11.2245	34.1699	43.8237	165.3929	0.5913	2
$M' = 40$	2.9838	8.5156	24.3029	28.5199	91.1597	0.6583	2
$M' = 50$	2.2512	6.5483	19.0471	22.9231	76.9016	0.6388	2
$s = 100$ (%)	**Q1**	**Q2**	**Q3**	**Mean**	**SD**	**AI**	**Censoring rate (%)**
$M' = 30$	2.6446	8.1882	25.3524	33.3320	131.5271	0.5735	3
$M' = 40$	2.2550	6.7768	20.3659	25.6420	93.5750	0.6048	2
$M' = 50$	1.6783	5.0637	15.2784	19.3458	71.3335	0.6003	2

Table 47 Descriptive statistics of R_t^s (First Quartile, Second Quartile (Median), Third Quartile, Mean, Standard Deviation, Asymmetry Index) and related censored units as a function of *s*, *M* and *M*′

Descriptive statistics of R_t^s-APPLE with $M = 80\%$							
$s = 0$ (%)	**Q1**	**Q2**	**Q3**	**Mean**	**SD**	**AI**	**Censoring rate (%)**
$M' = 30$	2.8495	14.9498	78.4341	306.2351	6.2655e+03	0.1395	12
$M' = 40$	2.6831	13.6672	69.6175	251.6335	4.6261e+03	0.1543	11
$M' = 50$	2.5477	12.7777	64.0845	222.6104	3.8719e+03	0.1626	11
$s = 5$ (%)	**Q1**	**Q2**	**Q3**	**Mean**	**SD**	**AI**	**Censoring rate (%)**
$M' = 30$	3.9719	11.1898	31.5239	36.3805	112.5476	0.6715	0.8
$M' = 40$	2.7016	6.7808	17.0197	17.1997	40.0940	0.7796	0.8
$M' = 50$	1.9236	4.1280	8.8586	7.8352	12.6401	0.8799	0.8
$s = 50$ (%)	**Q1**	**Q2**	**Q3**	**Mean**	**SD**	**AI**	**Censoring rate (%)**
$M' = 30$	3.2737	8.1645	20.3619	20.4437	46.9310	0.7849	0
$M' = 40$	2.6989	6.3796	15.0796	14.3884	29.0873	0.8260	0
$M' = 50$	2.0327	4.3645	9.3711	8.2915	13.3931	0.8796	0
$s = 100$ (%)	**Q1**	**Q2**	**Q3**	**Mean**	**SD**	**AI**	**Censoring rate (%)**
$M' = 30$	4.0080	11.3441	32.1078	32.2761	116.6773	0.6668	1.6
$M' = 40$	2.8912	7.7920	21.0002	22.9520	63.5914	0.7152	1.6
$M' = 50$	2.1594	5.7150	15.1256	16.1873	42.8962	0.7324	1.6

Table 48 Descriptive statistics of S_r^s (First Quartile, Second Quartile (Median), Third Quartile, Mean, Standard Deviation, Asymmetry Index) and related censored units as a function of s, M and M'

Descriptive statistics of S_r^s-TESLA with $M = 80\%$							
$s = 0$ (%)	**Q1**	**Q2**	**Q3**	**Mean**	**SD**	**AI**	**Censoring rate (%)**
$M' = 30$	0.0101	0.0436	0.2083	0.0687	0.0987	0.7629	9
$M' = 40$	0.0099	0.0382	0.1667	0.0584	0.0800	0.7570	8
$M' = 50$	0.0092	0.0317	0.1250	0.0465	0.0607	0.7336	6
$s = 5$ (%)	**Q1**	**Q2**	**Q3**	**Mean**	**SD**	**AI**	**Censoring rate (%)**
$M' = 30$	0.0303	0.0774	0.2083	0.0979	0.1043	0.5894	0.8
$M' = 40$	0.0472	0.1167	0.3000	0.0986	0.0883	-0.6153	0
$M' = 50$	0.0675	0.1250	0.2250	0.0998	0.0657	-1.1503	0
$s = 50$ (%)	**Q1**	**Q2**	**Q3**	**Mean**	**SD**	**AI**	**Censoring rate (%)**
$M' = 30$	0.0189	0.0528	0.1458	0.0826	0.0963	0.9287	0.8
$M' = 40$	0.0297	0.0733	0.1667	0.0865	0.0805	0.4914	0
$M' = 50$	0.0317	0.0675	0.2250	0.0757	0.0643	0.3843	0
$s = 100$ (%)	**Q1**	**Q2**	**Q3**	**Mean**	**SD**	**AI**	**Censoring rate (%)**
$M' = 30$	0.0196	0.0528	0.1458	0.0837	0.0986	0.9409	0.8
$M' = 40$	0.0258	0.0619	0.1667	0.0812	0.0836	0.6938	0.8
$M' = 50$	0.0240	0.0675	0.2250	0.0653	0.0649	-0.1007	0.8

Table 49 Descriptive statistics of S_r^s (First Quartile, Second Quartile (Median), Third Quartile, Mean, Standard Deviation, Asymmetry Index) and related censored units as a function of s, M and M'

Descriptive statistics of S_r^s-NETFLIX with $M = 80\%$							
$s = 0$ (%)	**Q1**	**Q2**	**Q3**	**Mean**	**SD**	**AI**	**Censoring rate (%)**
$M' = 30$	0.0958	0.0323	0.2083	0.0588	0.0954	0.8335	11
$M' = 40$	0.0050	0.0276	0.1667	0.0481	0.0768	0.8005	10
$M' = 50$	0.0039	0.0207	0.1250	0.0364	0.0577	0.8137	10
$s = 5$ (%)	**Q1**	**Q2**	**Q3**	**Mean**	**SD**	**AI**	**Censoring rate (%)**
$M' = 30$	0.0130	0.0436	0.1458	0.0730	0.0966	0.9153	2
$M' = 40$	0.0157	0.0472	0.1667	0.0679	0.0818	0.7576	1.6
$M' = 50$	0.0207	0.0550	0.2250	0.0611	0.0648	0.2843	0.8
$s = 50$ (%)	**Q1**	**Q2**	**Q3**	**Mean**	**SD**	**AI**	**Censoring rate (%)**
$M' = 30$	0.0145	0.0436	0.1458	0.0753	0.0954	0.9989	2
$M' = 40$	0.0163	0.0472	0.1167	0.0686	0.0798	0.8023	2
$M' = 50$	0.0154	0.0464	0.1250	0.0561	0.0629	0.4591	2
$s = 100$ (%)	**Q1**	**Q2**	**Q3**	**Mean**	**SD**	**AI**	**Censoring rate (%)**
$M' = 30$	0.0196	0.0590	0.2083	0.0847	0.1018	0.7565	3
$M' = 40$	0.0195	0.0619	0.1667	0.0729	0.0837	0.3939	2
$M' = 50$	0.0194	0.0550	0.2250	0.0589	0.0652	0.1809	2

Table 50 Descriptive statistics of S_r^s (First Quartile, Second Quartile (Median), Third Quartile, Mean, Standard Deviation, Asymmetry Index) and related censored units as a function of s, M and M'

Descriptive statistics of S_r^s-APPLE with $M = 80\%$							
$s = 0$ (%)	**Q1**	**Q2**	**Q3**	**Mean**	**SD**	**AI**	**Censoring rate (%)**
$M' = 30$	0.0064	0.0345	0.2083	0.0603	0.0959	0.8062	12
$M' = 40$	0.0058	0.0297	0.1667	0.0498	0.0776	0.7768	11
$M' = 50$	0.0047	0.0240	0.1250	0.0381	0.0587	0.7203	11
$s = 5$ (%)	**Q1**	**Q2**	**Q3**	**Mean**	**SD**	**AI**	**Censoring rate (%)**
$M' = 30$	0.0159	0.0436	0.1458	0.0762	0.0933	1.0486	0.8
$M' = 40$	0.0229	0.0619	0.1667	0.0783	0.0812	0.6074	0.8
$M' = 50$	0.0354	0.0675	0.2250	0.0764	0.0643	0.4164	0.8
$s = 50$ (%)	**Q1**	**Q2**	**Q3**	**Mean**	**SD**	**AI**	**Censoring rate (%)**
$M' = 30$	0.0244	0.0590	0.1458	0.0903	0.0970	0.9669	0
$M' = 40$	0.0258	0.0619	0.1667	0.0821	0.0809	0.7501	0
$M' = 50$	0.0317	0.0675	0.1250	0.0750	0.0637	0.3517	0
$s = 100$ (%)	**Q1**	**Q2**	**Q3**	**Mean**	**SD**	**AI**	**Censoring rate (%)**
$M' = 30$	0.0154	0.0436	0.1125	0.0756	0.0931	1.0335	1.6
$M' = 40$	0.0186	0.0536	0.1667	0.0723	0.0803	0.6994	1.6
$M' = 50$	0.0194	0.0550	0.1250	0.0612	0.0635	0.2911	1.6

Table 51 Kullback–Leibler divergence computed on the risk measure T_c^s as a function of M and s for Tesla, Netflix and Apple

Kullback-Leibler divergence for T_c^s			
$s = 0$	**$D(P\|Q)$**	**$D(P\|Q)$**	**$D(P\|Q)$**
$M = 30\%$	**0.8473**	**0.2776**	1.8671
$M = 40\%$	0.9402	0.3344	1.4934
$M = 80\%$	1.1248	0.4784	**1.3141**
$s = 5$	**$D(P\|Q)$**	**$D(P\|Q)$**	**$D(P\|Q)$**
$M = 30\%$	**0.1221**	0.1993	0.1044
$M = 40\%$	0.2544	**0.1881**	**0.0018**
$M = 80\%$	0.2100	0.2124	0.0052
$s = 50$	**$D(P\|Q)$**	**$D(P\|Q)$**	**$D(P\|Q)$**
$M = 30\%$	0.0795	**0.1045**	0.0463
$M = 40\%$	**0.0108**	0.1629	0.0387
$M = 80\%$	0.0147	0.2471	**0.0118**
$s = 100$	**$D(P\|Q)$**	**$D(P\|Q)$**	**$D(P\|Q)$**
$M = 30\%$	0.2625	**0.0153**	0.0339
$M = 40\%$	0.1066	0.0314	0.0223
$M = 80\%$	**0.0684**	0.1581	**0.0220**

The smallest distances for each s are in bold

Table 52 Kullback–Leibler divergence computed on the risk measure R_t^s as a function of M, M' and s for Tesla, Netflix and Apple

Kullback–Leibler divergence for R_t^s with $M = 80\%$			
$s = 0$	**$D(P\|Q)$**	**$D(P\|Q)$**	**$D(P\|Q)$**
$M' = 30\%$	0.2660	**0.1734**	**0.0971**
$M' = 40\%$	0.0466	0.2530	0.1832
$M' = 50\%$	**0.0186**	0.4686	0.6976
$s = 5$	**$D(P\|Q)$**	**$D(P\|Q)$**	**$D(P\|Q)$**
$M' = 30\%$	0.4531	**0.0345**	0.1690
$M' = 40\%$	**0.4227**	0.0402	**0.1428**
$M' = 50\%$	0.7375	0.1053	0.2298
$s = 50$	**$D(P\|Q)$**	**$D(P\|Q)$**	**$D(P\|Q)$**
$M' = 30\%$	0.0665	0.0155	0.0595
$M' = 40\%$	0.1448	**0.0037**	**0.0423**
$M' = 50\%$	**0.0160**	0.0210	0.0595
$s = 100$	**$D(P\|Q)$**	**$D(P\|Q)$**	**$D(P\|Q)$**
$M' = 30\%$	**0.0225**	0.0686	0.0049
$M' = 40\%$	0.0259	**0.0661**	**0.0042**
$M' = 50\%$	0.0321	0.0910	0.0117

The smallest distances for each s are in bold

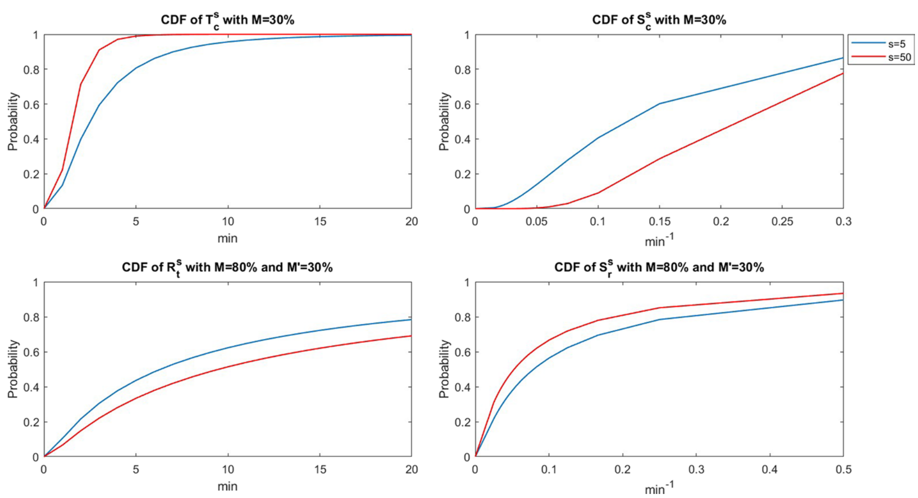

Fig. 3 Cumulative distribution functions (CDFs) on the first 20 min of the trading day for T_c^s, S_c^s, R_t^s, and S_r^s. All the blue lines represent the CDFs for scenario $s = 0$ while, the red lines are the CDFs for scenario $s = 100$

Our long-term objective is to jointly examine volumes and returns using the multivariate WISMC model described in D'Amico and Petroni (2021). In order to confirm the efficacy of our model, we also wish to compare the outcomes of the WISMC model with those of inflated econometric models, such as the autoregressive moving average and generalized autoregressive conditional heteroskedasticity models.

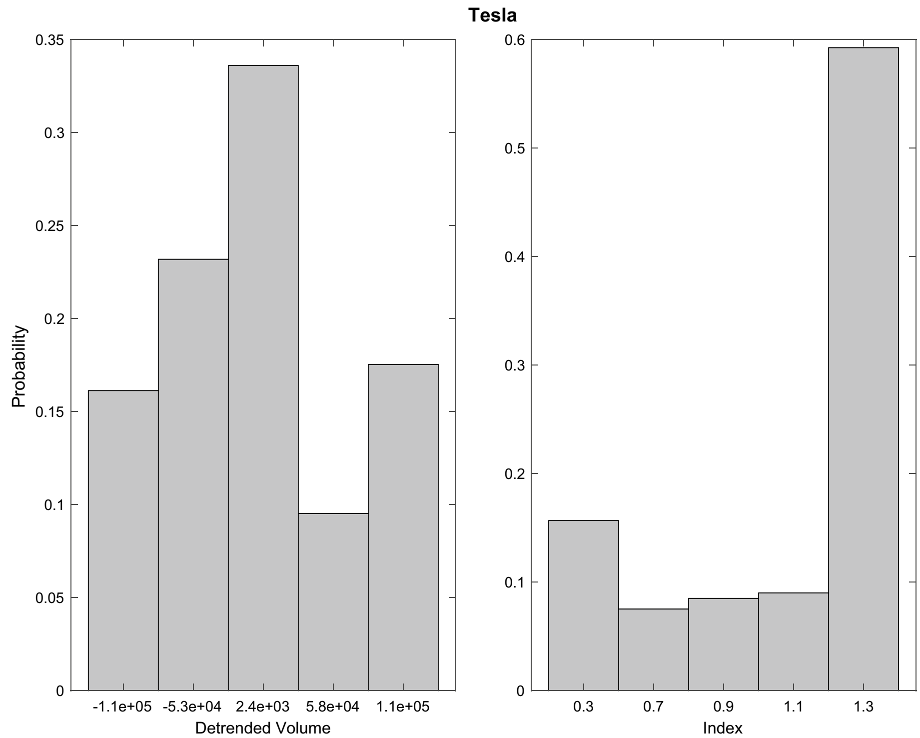

Fig. 4 Probability plots for both the detrended volume states and index states for Tesla asset

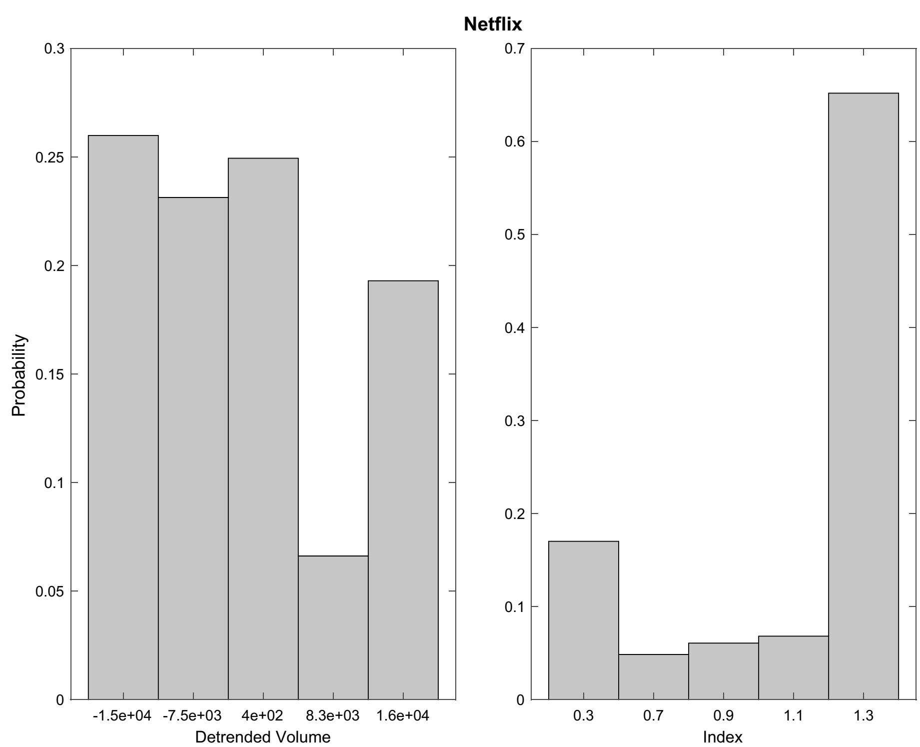

Fig. 5 Probability plots for both the detrended volume states and index states for Netflix asset

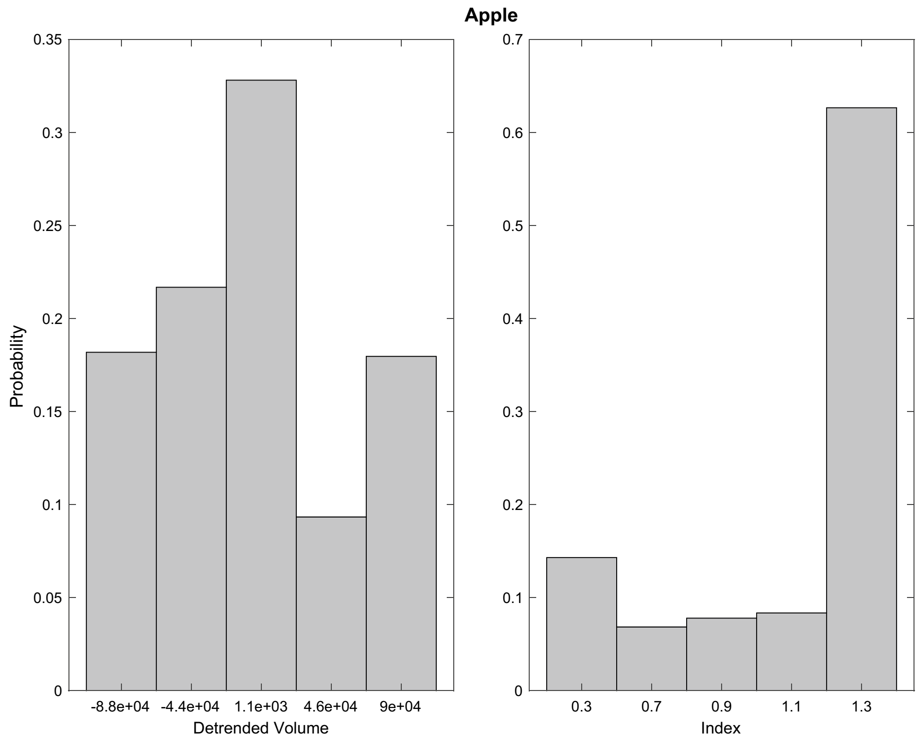

Fig. 6 Probability plots for both the detrended volume states and index states for Apple asset

Acknowledgements
The authors are grateful to the journal's associate editor and anonymous referees for their extremely useful suggestions to improve the quality of the article.

Author Contributions
All authors read and approved the final manuscripts. They equally contributed to this research paper.

Funding
The authors declare the absence of funding.

Availability of data and materials
The authors declare that the dataset used and analysed during the current study is available from the corresponding author on reasonable request.

Declarations

Competing interests
The authors declare that they have no competing interests.

Received: 18 March 2023 Accepted: 18 December 2023
Published online: 22 February 2024

References

Bank M, Larch M, Peter G (2011) Google search volume and its influence on liquidity and returns of german stocks. Fin Markets Portfolio Mgmt 25:239–264

Barbu VS, Limnios N (2009) Semi-Markov chains and hidden semi-Markov models toward applications: their use in reliability and DNA analysis. Springer, Berlin

Cantor R (2001) Moody's investors service response to the consultative paper issued by the basel committee on bank supervision "a new capital adequacy framework". J Bank Financ 25(1):171–185

Casati A, Tabachnik S (2013) The statistics of the maximum drawdown in financial time series. Advances in Financial Risk Management: Corporates, Intermediaries and Portfolios, 347–363

Chekhlov A, Uryasev S, Zabarankin M (2005) Drawdown measure in portfolio optimization. Int J Theor Appl Financ 8(01):13–58

D'Amico G, Petroni F (2011) A semi-markov model with memory for price changes. J Stat Mech Theory Exp 2011(12):12009
D'Amico G, Petroni F (2012) A semi-markov model for price returns. Phys A 391(20):4867–4876
D'Amico G, Petroni F (2012) Weighted-indexed semi-markov models for modeling financial returns. J Stat Mech Theory Exp 2012(07):07015
D'Amico G, Petroni F (2018) Copula based multivariate semi-markov models with applications in high-frequency finance. Eur J Oper Res 267(2):765–777
D'Amico G, Petroni F (2021) A micro-to-macro approach to returns, volumes and waiting times. Appl Stoch Model Bus Ind 37(4):767–789
D'Amico G, Petroni F, Prattico F (2013) Wind speed modeled as an indexed semi-markov process. Environmetrics 24(6):367–376
D'Amico G, Di Basilio B, Petroni F (2020) A semi-markovian approach to drawdown-based measures. Adv Complex Syst 23(08):2050020
D'Amico G, Di Basilio B, Petroni F, Gismondi F (2023) An econometric analysis of drawdown based measures. In: Stochastic processes, statistical methods, and engineering mathematics: SPAS 2019, Västerås, Sweden, September 30–October 2, pp. 489–510. Springer
D'Amico G, Gismondi F, Petroni F (2018) A new approach to the modeling of financial volumes. In: Stochastic processes and applications: SPAS2017, Västerås and Stockholm, Sweden, pp. 363–373. Springer
De Blasis R (2023) Weighted-indexed semi-markov model: calibration and application to financial modeling. Financ Innov 9(1):1–16
Goldberg LR, Mahmoud O (2017) Drawdown: from practice to theory and back again. Math Financ Econ 11:275–297
Graczyk MB, Duarte Queiros SM (2016) Intraday seasonalities and nonstationarity of trading volume in financial markets: individual and cross-sectional features. PLoS ONE 11(11):0165057
Hongzhong Z. Stochastic Drawdowns. World Scientific
Janssen J (2013) Semi-Markov models: theory and applications. Springer, Berlin
Jiang Y (2022) Credit ratings, financial ratios, and equity risk: a decomposition analysis based on moody's, standard & poor's and fitch's ratings. Financ Res Lett 46:102512
Kaplan EL, Meier P (1958) Nonparametric estimation from incomplete observations. J Am Stat Assoc 53(282):457–481
Koukoumis C, Karagrigoriou A (2021) On entropy-type measures and divergences with applications in engineering, management and applied sciences. Int J Math Eng Manag Sci 6(3):688
Kullback S, Leibler RA (1951) On information and sufficiency. Ann Math Stat 22(1):79–86
Limnios N, Oprisan G (2001) Semi-Markov processes and reliability. Springer, Berlin
Li L, Zeng P, Zhang G (2022) Speed and duration of drawdown under general markov models. Available at SSRN 4222362
Martınez MA, Nieto B, Rubio G, Tapia M (2005) Asset pricing and systematic liquidity risk: An empirical investigation of the spanish stock market. Int Rev Econ Financ 14(1):81–103
Masala G, Petroni F (2022) Drawdown risk measures for asset portfolios with high frequency data. Ann Financ 19:265
Pasricha P, Selvamuthu D, D'Amico G, Manca R (2020) Portfolio optimization of credit risky bonds: a semi-markov process approach. Financ Innov 6(1):1–14
Puneet P, Dharmaraja S (2021) A markov regenerative process with recurrence time and its application. Financ Innov 7(1):1
Queirós SD (2005) On the emergence of a generalised gamma distribution application to traded volume in financial markets. Europhys Lett 71(3):339
Queirós SMD (2016) Trading volume in financial markets: an introductory review. Chaos Solitons Fractals 88:24–37
Song K-S (2002) Goodness-of-fit tests based on kullback-leibler discrimination information. IEEE Trans Inf Theory 48(5):1103–1117
Swishchuk A, Islam MS (2011) The geometric markov renewal processes with application to finance. Stoch Anal Appl 29(4):684–705
Swishchuk A, Vadori N (2017) A semi-markovian modeling of limit order markets. SIAM J Financ Math 8(1):240–273
Vassiliou P-C (2014) Semi-markov migration process in a stochastic market in credit risk. Linear Algebra Appl 450:13–43
Vassiliou P-C (2020) Non-homogeneous semi-markov and markov renewal processes and change of measure in credit risk. Mathematics 9(1):55
Zhang H, Hadjiliadis O (2012) Drawdowns and the speed of market crash. Methodol Comput Appl Probab 14:739–752
Zhang X, Huang Y, Xu K, Xing L (2023) Novel modelling strategies for high-frequency stock trading data. Financ Innov 9(1):1–25

Publisher's Note